

Abstract

FESSELIN, AN INTRINSICALLY DISORDERED SMOOTH MUSCLE PROTEIN, ORGANIZES AND STABILIZES ACTIN-MYOSIN AND MYOSIN

By

Nathaniel Kingsbury

November 2014

Committee Chair: Joseph M. Chalovich

Department: Biochemistry and Molecular Biology

Fesselin is an intrinsically disordered protein that is known to bind a large variety of cytoskeletal proteins. The proteins fesselin is known to bind include: actin (Leinweber et al. 1999), α -actinin (Pham et al. 2006), calmodulin (Schroeter et al. 2004), filamin (Weins et al. 2001), and smooth myosin (Schroeter et al. 2005). The binding of fessilin to smooth myosin is of particular interest because unphosphorylated smooth muscle myosin filaments are unstable in the presence of ATP (Trybus et al. 1982, Ikebe et al. 1983, Suzuki et al. 1978). However, in smooth muscle cells unphosphorylated myosin filaments are maintained (Milton et al. 2011). Several proteins have been identified that stabilize myosin filaments and actin-myosin filament interactions. Our experiments show that fesselin may be one such protein.

The organization of F-actin and myosin filaments by fesselin was observed by monitoring the rate of dissociation of actin-myosin by ATP in a stopped-flow device. Actin-myosin dissociation was measured by light scattering (a measure of particle size) and by pyrene-actin or acrylodan-tropomyosin fluorescence (a measure of myosin-actin bond breaking). The stopped-flow studies were further supported with electron

microscopy analysis. These experiments showed that fesselin was able to tether actin and myosin filaments together without significantly impacting the rate of the actin-myosin bond breaking.

The stabilization of myosin filaments by fesselin was tested using a similar method. First, stopped-flow rapid kinetics was used to measure the rate of ATP induced myosin filament break down. Next, electron microscopy was used to support the stopped-flow data and observe the effects of fesselin on myosin filament organization. Through the stopped-flow and electron microscopy experiments it was found that fesselin stabilizes myosin filaments. The electron microscopy experiments further revealed that fesselin enhanced myosin filament size and organized them into bundles.

Previously published results showed that the interaction between fesselin and actin is regulated by calmodulin (Schroeter et al. 2004). The final set of experiments presented here examined the possibility that calmodulin regulates the interactions between fesselin and myosin. The calmodulin regulation of fesselin myosin interactions would greatly expand the role that fesselin has within smooth muscle by placing it within the calcium signaling pathway. The regulation of fesselin-myosin interactions by calmodulin was tested using pyrene labeled actin as well as N,N'-Dimethyl-N-(Iodoacetyl)-N'-(7-Nitrobenz-2-Oxa-1,3-Diazol-4-yl)Ethylenediamine labeled fesselin (IANBD-fesselin). These experiments showed that the interactions between fesselin and myosin are regulated by calmodulin. Overall, our results support that fesselin plays a critical role within smooth muscle to organize contractile elements.

FESSELIN, AN INTRINSICALLY DISORDERED SMOOTH MUSCLE PROTEIN,
ORGANIZES AND STABILIZES ACTIN-MYOSIN AND MYOSIN

A Thesis

Presented To the Faculty of the Department of Biochemistry and Molecular Biology
East Carolina University

In Partial Fulfillment of the Requirements for the Master's of Science degree in
Biomedical Sciences

by

Nathaniel Kingsbury

November, 2014

© Nathaniel Kingsbury, 2014

FESSELIN AN INTRINSICALLY DISORDERED SMOOTH MUSCLE PROTEIN
ORGANIZES AND STABILIZES ACTIN-MYOSIN AND MYOSIN

by

Nathaniel Kingsbury

APPROVED BY:

DIRECTOR OF THESIS: _____
Dr. Joseph Chalovich, PhD

COMMITTEE MEMBER: _____
Dr. Brian Shewchuk, PhD

COMMITTEE MEMBER: _____
Dr. Tonya Zeczycki, PhD

COMMITTEE MEMBER: _____
Dr. David Brown, PhD

CHAIR OF THE DEPARTMENT
OF BIOCHEMISTRY: _____
Dr. Phillip Pekala, PhD

DEAN OF THE
GRADUATE SCHOOL: _____
Paul J. Gemperline, PhD

Table of Contents

List of Figures	v
List of Abbreviations.....	viii
Introduction.....	1
Fesselin is an intrinsically disordered protein	1
Disease related roles of fesselin	2
Cellular localization of fesselin is consistent with a role in actin organization	3
Fesselin polymerizes and bundles actin.....	4
Fesselin binding to myosin suggests a broader role within smooth muscle.....	4
Smooth muscle myosin conformations and filament formation.....	5
Smooth muscle myosin is stabilized by several proteins in smooth muscle.....	10
Several proteins are known to cross-link actin and myosin.....	11
HYPOTHESIS: Fesselin binds to and organizes smooth myosin and holds actin and myosin together.....	12
Materials and Methods	16
Fesselin preparation	16
Fesselin purification method 2.....	18
Smooth muscle myosin preparation.....	23
Actin preparation	24

Myosin and calmodulin affinity columns	26
Fluorescent labeled proteins	27
IANBD fesselin.....	27
Acrylodan tropomyosin.....	28
Pyrene actin	29
Protein cross-linking.....	30
Protein co-sedimentation	31
Transient kinetics	32
The state of unphosphorylated smooth muscle myosin	35
Electron microscopy.....	38
ATP grids.....	39
ATP free grids.....	39
Grid visualization	39
Results	42
Part I The interactions of fesselin with actin-myosin and myosin	42
Fesselin reduces the rate of dissociation of myosin and actin by ATP.....	46
Electron microscopy shows fesselin stabilizing actin and myosin against ATP	47
Fesselin stabilizes actin-myosin by tethering both proteins together and not by reducing the detachment rate from the specific actin-myosin interface.....	50
Fesselin stabilizes myosin filaments	66
Fesselin increases the length and thickness of myosin filaments	73

Part II. Determination of sites of interaction of fesselin and myosin.....	79
Identification of binding sites for the fesselin-myosin interaction.....	79
Covalent Cross-linking fesselin and myosin	79
Fesselin peptide co-sedimentation.....	88
Part III: Regulation of fesselin-myosin binding	94
The effect of calmodulin on actin and myosin dissociation.....	94
IANBD fesselin binding to myosin fragments.....	100
Discussion	110
Fesselin stabilizes myosin	111
Fesselin organizes actin-myosin.....	112
The activities of fesselin are regulated by calcium calmodulin	117
The role of fesselin within the cell.....	119
Conclusions.....	120
Future Directions.....	120
References	122
Appendix A: Reduction of actin-myosin dissociation by caldesmon compared to fesselin	126
Appendix B: Permission letter	129

List of Figures

Figure 1 The regulation of smooth muscle myosin includes conformational shifts of the myosin	6
Figure 2 A simplified schematic of Smooth muscle regulation	8
Figure 3 Chart of proposed activities of fesselin with actin and myosin	14
Figure 4 Fesselin purification requires multiple steps	20
Table 1 Fluorescent probes used	33
Figure 5 MANT-ATP measurements were able to show that the myosin used was regulated properly for unphosphorylated smooth myosin	36
Figure 6 The use of negative and positive stain electron microscopy gave different information for the same samples.....	41
Figure 7 Fesselin increased the resistance of actin-myosin filaments against ATP dissociation	45
Figure 8 Electron microscopy images showing myosin filaments binding along actin filaments in the presence of ATP only when fesselin is present	48
Figure 9 Myosin can be digested with proteases into several fragments with differing functions	52
Figure 10 Fesselin had only slight effects on HMM dissociation from actin	54
Figure 11 Fluorescence transients for 0.2 μ M phalloidin-pyrene-actin with 0.05 μ M smooth myosin with and without fesselin	57
Figure 12 Fluorescein-smooth myosin measurements were unable to monitor actin-myosin dissociation	60

Figure 13 Fesselin had little effect on acrylodan tropomyosin fluorescence following the rapid addition of ATP to the actin–myosin complex.....	64
Figure 14 Fesselin reduces the rate of ATP-induced, smooth muscle myosin dissociation	68
Figure 15 Fesselin enhanced ATP resistance of myosin filaments shown using electron microscopy.....	71
Figure 16 Electron microscopic analysis shows fesselin increases the length and width of smooth muscle myosin filaments	75
Figure 17 Fesselin bundled myosin filaments into large arrays	77
Figure 18 Cross-linking of myosin and fesselin did not yield definitive results	82
Figure 19 Using agarose-acrylamide gels the myosin-fesselin complexes were hoped to be resolved	84
Figure 20 The myosin used in the cross-linking contains disulfide-linked myosin	86
Figure 21 Co-sedimentation of intact smooth myosin and fesselin peptides acted to purify remaining intact fesselin in the samples	90
Figure 22 Using myosin and myosin fragments for affinity purification of fesselin fragments proved to be difficult.....	92
Figure 23 Stopped-flow traces demonstrating the changes induced by calmodulin on actin-fesselin-myosin dissociation.....	96
Figure 24 Calmodulin reduces the rate of breaking the actin-myosin bond in pyrene-labeled actin-fesselin-myosin in the presence calcium and increases the rate in the absence of calcium	98
Figure 25 Binding of IANBD-labeled fesselin to myosin in the presence of calmodulin.....	102

Figure 26 Light scattering measurements of myosin bundling by fesselin in the presence of calmodulin.....	104
Figure 27 Scheme used for the modeling of IANBD-fesselin fluorescence changes induced by Ca ²⁺ -calmodulin	106
Figure 28 Using IANBD-fesselin the binding kinetics to both smooth myosin subfragment-1 (S-1) and intact smooth myosin were observed	108
Figure 29 Schematic representation of the actin-fesselin-myosin interaction.....	115
Figure 30 A simplified schematic of smooth muscle regulation with the additional fesselin-myosin regulation.....	119
Figure 31 Proposed activities of fesselin with actin and myosin	123
Figure 32 Fesselin slows the dissociation of actin-myosin by ATP to a greater extent than caldesmon	130

List of Abbreviations

1. Pyrene - N-(1-Pyrene)Iodoacetamide
2. MANT-ATP - 2'(3')-O-(*N*-methylantraniloyl)-ATP
3. Acrylodan - 6-Acryloyl-2-Dimethylaminonaphthalene
4. IANBD - N,N'-Dimethyl-N-(Iodoacetyl)-N'-(7-Nitrobenz-2-Oxa-1,3-Diazol-4-yl)Ethylenediamine
5. S-1 – Myosin subfragment-1
6. EDC - 1-Ethyl-3-(3-dimethylaminopropyl) carbodiimide
7. NHS - N-Hydroxysuccinimide
8. DTSSP - 3,3'-dithiobis(sulfosuccinimidylpropionate)
9. PPDM - N,N'-1,4-Phenylene-dimaleimide
10. DMDTPP - Dimethyl 3,3'-dithiopropionimidate dihydrochloride
11. SASD - Sulfosuccinimidyl-2-(*p*-azidosalicylamido)ethyl-1,3-dithiopropionate
12. MOPS - 3-(*N*-morpholino)propanesulfonic acid
13. EDTA - Ethylenediaminetetraacetic acid
14. DTT – Dithiothreitol

Introduction

Within humans there are three major types of muscle: skeletal, cardiac, and smooth. Skeletal and cardiac muscles have striations that result from the highly ordered myosin and actin filaments. The structural organization of actin and myosin in smooth muscle and non-muscle cells is less obvious. However, it is certain, that myosin and actin must exist in their filamentous states and these filaments must be in close physical proximity to each other for contraction to occur. Striated muscles contain a bevy of proteins that stabilize and organize the filaments. There is also a group of proteins within smooth and non-muscle cells that organize actin and myosin and hold them in close association with each other. We propose that the protein fesselin, discovered in our laboratory, stabilizes actin and myosin filament and organizes these filaments into contractile units.

Fesselin is an Intrinsically Disordered Protein

Fesselin was first isolated from avian smooth muscle (Leinweber et al. 1999, Schroeter et al. 2008). Fesselin is proline rich protein with a pI near 9.3 (Leinweber et al. 1999). The proline residues and negatively charged residues produce a protein that is intrinsically disordered (Khaymina et al. 2007).

Intrinsically disordered proteins (IDP) typically have roles in signaling, transcription, and chromatin remodeling. This type of protein can also provide flexible linkers between parts of a complex, and the IDP act as adaptors for their ligands.

To visualize an intrinsically disordered protein, such as fesselin, one could picture a length of rope, while a typically structured protein can be thought of as a basket. Following this analogy, the target ligands can be thought of as group of sticks of various lengths. The basket, or typically structured protein, could be used to quickly and easily hold some of the sticks, as long as they are of short enough length to fit inside. For the sticks that are too large, a whole new basket would be needed. In the case of our intrinsically disordered protein, or rope, any of the sticks can be carried regardless of length, but it would require more time to gather the sticks and lash them together. Typically structured proteins are adept at dealing with their target ligand but have a smaller range of targets. Intrinsically disordered proteins require more time and energy to bind their ligands. This is due to the fact that many intrinsically disordered proteins undergo folding as they bind their target. This fact allows intrinsically disordered proteins to have a large range of ligands. Fesselin is known to bind to actin (Leinweber et al. 1999) desmin (Renegar et al. 2009), α -actinin (Pham et al. 2006), zyxin (Linnemann 2010), calmodulin (Schroeter et al. 2004, Kolakowski et al. 2004), and smooth muscle myosin (Schroeter et al. 2005). This list of binding partners is likely to grow.

Disease related roles of fesselin

Other labs have shown that isoforms of fesselin play roles within cancer metastasis. When fesselin isoforms are found in the cytoplasm of cancer cells, it correlates with more metastatic cancer (Stevenson et al. 2012). These studies found the

heightened metastatic behavior was due to the promotion of actin bundle formation (Kai et al. 2013, Stevenson et al. 2012).

The heightened metastatic behavior of cancer cells with fesselin seems to be due to an up regulation of fesselin leading to more organized contractile systems and thus more motility. The opposite is true for the interactions of fesselin isoforms and duchenne muscular dystrophy (DMD). Within skeletal muscle cells cultured from patients with DMD, the expression of the human skeletal isoform of fesselin is down regulated (Tkatchenko et al. 2001).

Like all forms of muscular dystrophy, DMD is caused by a lack of organization of the muscle tissue. The disruption of organization is caused by problems with expression or activity of dystrophin. DMD is one of the most common forms of muscular dystrophy as well as the most severe. The decrease in the skeletal isoform of fesselin may be related to the severity of Duchenne muscular dystrophy. Previous groups found that the skeletal isoform of fesselin is expressed very early in differentiating muscle cells and likely plays a critical role in actin organization (Linnemann et al. 2010).

Cellular Localization of Fesselin is consistent with a role in actin organization.

Antibody-staining of avian smooth muscle tissue revealed that fesselin was localized to the dense bodies (Renegar et al. 2009). Within smooth muscle the dense bodies are the actin organizing centers that connect the contractile actin filaments to the cell membrane. Through these structures the force produced by myosin filaments sliding along actin filaments translates to movement of the cell.

Fesselin polymerizes and bundles actin

The localization of fesselin to the dense bodies of smooth muscle showed that fesselin likely plays a critical role in F-actin filament organization. To polymerize F-actin filaments one F-actin monomer needs to bind with two other F-actin monomers to form an actin nuclei for filament growth. The formation of actin nuclei is the rate-limiting step for F-actin filament polymerization.

Fesselin binds actin monomers, and aids in its polymerization to F-actin filaments by stabilizing the actin nuclei (Beall et al. 2001, Leinweber et al. 1999). In addition fesselin was also shown to bundle F-actin filaments together (Schroeter et al. 2013). F-actin bundles are a required structure to make contraction possible as the bundles form a rigid support for the myosin to apply force.

The next finding involving fesselin and actin was the regulation of actin polymerization in the presence of calmodulin. Experiments were performed using pyrene-labeled-actin with fesselin and calmodulin. In these studies it was found that the polymerization of G-actin to F-actin filaments by fesselin was regulated by calmodulin (Schroeter et al. 2004, Kolakowski et al. 2004).

Fesselin binding to myosin suggests a broader role within smooth muscle

Dr. Schroeter observed that fesselin displaced myosin from actin (Schroeter et al. 2005). This is a common observation for actin binding proteins because they typically bind at a common site near the target-binding cleft of actin between domains 1 and 3 (Dominguez et al. 2011). Dr. Schroeter also observed evidence that fesselin bound directly to myosin, at a ratio of two myosin to one fesselin (Schroeter et al. 2005). The

direct binding to multiple myosin molecules by fesselin expanded the possible role for fesselin from an actin binding protein to one that organized the contractile apparatus of the cell.

Because of the requirement for proteins to stabilize actin-myosin interactions in relaxed muscle, we tested the possibility that fesselin organized contractile elements composed of both actin and myosin. That is, we investigated the possibility that fesselin stimulates the formation of actin bundles from G-actin, stabilizes myosin filaments and stabilizes actin bundle-myosin bundle associations. Investigating the function of fesselin in smooth muscle myosin is complex because this myosin is regulated by phosphorylation and forms inactive and active structures.

Smooth muscle myosin conformations and filament formation

In smooth muscle, the activity of myosin is modulated by the phosphorylation state of the regulatory light chains. Figure 1 shows a representation of the regulation of the smooth myosin conformational shift. Phosphorylation of the regulatory light chain of smooth myosin promotes the 6S conformer and thus the formation of myosin filaments. The calcium-signaling pathway (figure 2) leads to the phosphorylation of smooth myosin light chains and formation of functional myosin filaments. Within non-muscle and some smooth muscle cells myosin filaments disassemble when contraction is not required.

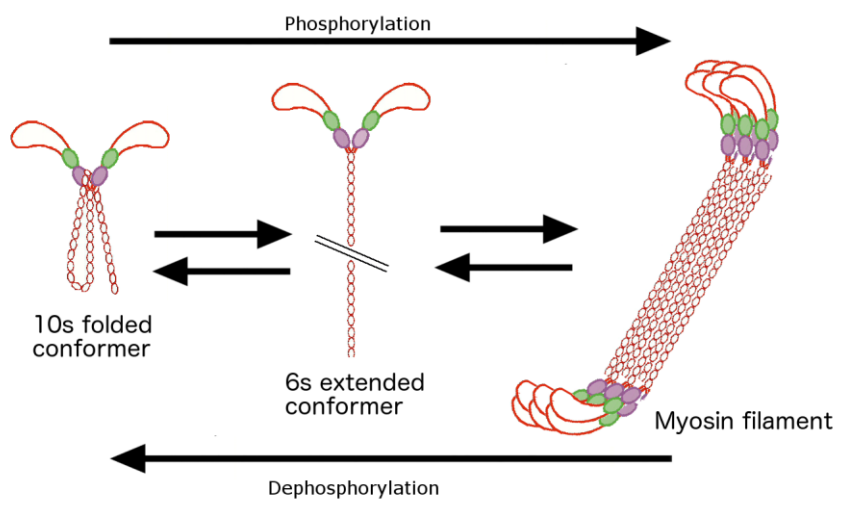


Figure 1

The regulation of smooth muscle myosin includes conformational shifts of the myosin. The conformation of smooth myosin determines the activity of the protein. Smooth myosin conformation is controlled mainly through two factors: ionic strength and phosphorylation state. The shift from 10s (inactive) to 6s (active) is promoted by lowering the ionic strength and/or phosphorylation of the light chains. Formation of myosin filaments requires moving to the 6s conformation. Increasing ionic strength or reducing the phosphorylation state of the myosin achieves shifting the equilibrium in the other direction.

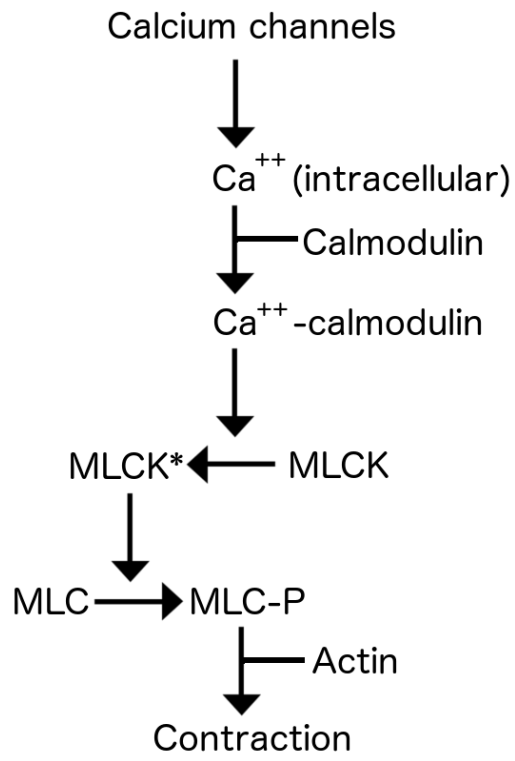


Figure 2

A simplified schematic of smooth muscle regulation. Calcium channels on the cell allow intracellular calcium ion increase. The calcium then binds to calmodulin. Calcium-calmodulin activates myosin light chain kinase (MLCK). Then MLCK phosphorylates the regulatory light chain of smooth myosin (MLC). The phosphorylation promotes myosin filament stability and the filament capable form of smooth myosin. The phosphorylated myosin can then more readily bind to actin leading to contraction.

Smooth muscle myosin is stabilized by several proteins in smooth muscle

As presented in figure 1 the formation of smooth myosin filaments is controlled through two major factors: phosphorylation of the regulatory light chains and ionic strength.

Smooth myosin forms filaments when the regulatory light chains are phosphorylated or when the ionic strength is near 0.15 M KCl (Trybus 1982). The presence of phosphorylated smooth myosin filaments in smooth muscle is unsurprising as phosphorylation promotes smooth myosin filament formation. A surprising finding was the presence of unphosphorylated myosin filaments within smooth muscle (Somylo et al. 1981). In vitro studies found that unphosphorylated smooth myosin filaments depolymerized in the presence of stoichiometric amounts of ATP (Onishi et al. 1978). It was noted that the myosin from filaments disassembled by ATP had a far lower ATPase rate than myosin disassembled by high salt (Suzuki et al. 1978). Other groups performed studies to monitor what changes occurred when ATP bound the myosin. It was found that upon binding to the unphosphorylated myosin, the ATP caused the myosin to disassemble into the inactive 10S conformation (Trybus et al. 1982). This finding was further confirmed by monitoring tryptophan fluorescence changes induced by ATP binding the myosin (Ikebe et al. 1983). The observation of unphosphorylated myosin filaments in smooth muscle taken into account with the in-vitro work leads to the conclusion that there is something stabilizing the unphosphorylated myosin filaments. The simple answer is an interaction between a myosin binding protein and the unphosphorylated smooth myosin that stabilizes the myosin filaments.

There have been several different proteins proposed to stabilize unphosphorylated smooth myosin filaments. Some proteins like telokin are proposed to

bind to 10S myosin and promote the transition to the 6S conformation (Kudryashov et al. 2002). The interaction of telokin with unphosphorylated smooth myosin aids in the formation of filaments and stabilizes the filaments against ATP-induced disassembly (Katayama et al. 1995). The interaction between telokin and smooth myosin is not unlike how myosin light chain kinase interacts with smooth myosin, this is because telokin is identical in structure to the C-terminus of myosin light chain kinase (Holden et al. 1992). Other proteins have been found to stabilize unphosphorylated smooth myosin filaments against ATP induced disassembly. One such protein is caldesmon (Katayama et al. 1995). Caldesmon was shown to bind several heavy meromyosin molecules together and stabilize myosin filaments (Marston et al. 1989). These observations lead to the conclusion that caldesmon binds across multiple smooth myosin molecules to stabilize the unphosphorylated smooth myosin filaments (Katayama et al. 1995).

We propose that fesselin interacts with smooth myosin in much the same way that caldesmon does, binding to myosin filaments and stabilizing them. The findings of Schroeter et al. support this method of interaction in that one fesselin binds to two myosin molecules (2005).

Several proteins are known to cross-link actin and myosin.

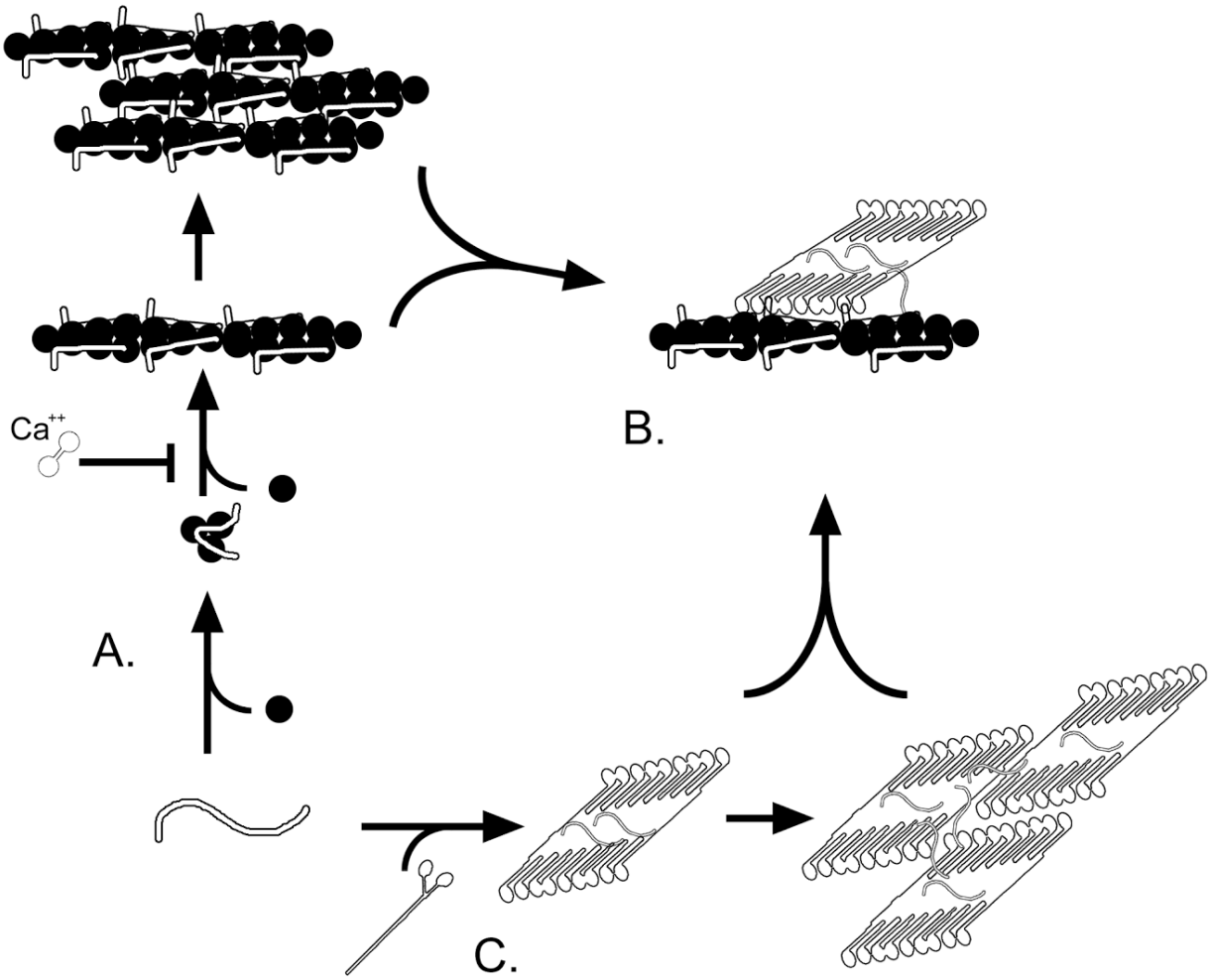
The direct linking between F-actin and myosin filaments is a simple way to keep the contractile filaments in association and organized for force production. There are a variety of proteins found within multiple muscle types that cross-link actin and myosin. Myosin-binding protein-C has been found to cross-link myosin and F-actin filaments together in striated muscle (Luther et al. 2011). This same cross-linking of actin and

myosin has been attributed to caldesmon as well as calponin in smooth muscle (Ikebe et al. 1988, Marston et al. 1992, Chalovich et al. 1988, Roman et al. 2013). The lack of a well-defined sarcomere within smooth muscle makes this cross-linking activity all the more important to the organization of actin and myosin filaments. This is because the sarcomere provides a rigid structure to hold the actin and myosin filaments in association. The cross-linking of F-actin and myosin filaments in smooth muscle is a viable solution to the organizational problem presented by a lack of a well-defined sarcomere. We propose that fesselin displays a similar activity to caldesmon and calponin by cross-linking F-actin and myosin filaments.

HYPOTHESIS: Fesselin binds to and organizes smooth myosin and holds actin and myosin together.

Because of its role in actin bundle formation and its binding to myosin, we propose that fesselin organizes smooth myosin and cross-links F-actin and myosin filaments. Figure 3 shows the proposed functions of fesselin alongside the previously known interactions. Figure 3 A shows the binding of fesselin to G-actin. The figure also shows formation of an F-actin nuclei and polymerization of F-actin filaments. This section further shows the formation of F-actin bundles from the filaments. Figure 3 B shows our proposed interaction between F-actin filaments and smooth myosin. This proposed interaction would fill the role of holding the actin and myosin filaments in association to facilitate productive contraction. Figure 3 C shows a proposed interaction between fesselin and smooth myosin alone. This takes into account the fesselin-actin

interactions and applies them to myosin. This proposed activity would aid in the organization of myosin filaments for contraction.



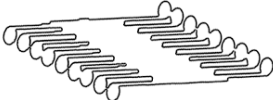
 Fesselin	 Smooth myosin filament
 Calcium calmodulin	 actin monomer
 Smooth myosin	 actin filament

Figure 3.

Proposed activities of fesselin with actin and myosin. A) Fesselin's known interactions with actin. Fesselin binds to actin and accelerates the polymerization, the acceleration is regulated by calcium calmodulin. The fesselin further interacts with actin filaments and bundles them. B) The proposed interaction between fesselin and actin-myosin. C) The proposed interactions of fesselin with myosin. This proposed activity is based on interactions of similar proteins and the affinity of fesselin for myosin.

Materials and Methods

Fesselin Preparation

The fesselin used in the studies presented here was isolated from frozen turkey gizzards. The gizzards were trimmed of connective tissue and diced into roughly one-inch pieces prior to freezing in liquid nitrogen. From the frozen gizzards two methods of fesselin preparation were compared.

The first method was based on the original procedure of Leinweber et al. (1999). 200 g of frozen turkey gizzards that were ground in a precooled meat grinder and transferred directly to a 1 L ice cold buffer (300 mM KCl, 50 mM MOPS pH 7.0, 0.5 mM Phenylmethanesulfonyl fluoride (PMSF), 0.75 mM bezamidine (0.12 g/L), soybean trypsin inhibitor, 5 mg leupeptin, protease inhibitor cocktail (0.5 mL prepared to manufacturer specifications SIGMA P2714).

The ground turkey gizzard mixture was then homogenized on ice in a Brinkmann homogenizer (model PCU7) 4 times for 10 seconds each. The homogeneous mixture was then heated in a 100° C water bath in 300-400 mL aliquots for 8 – 9 minutes while stirring. Heating continued until the mixture had separated into two layers.

After heat treatment, the mixture was moved to a pre-cooled vessel on ice and rapidly cooled. After 15 minutes, further protease inhibitors were added (SIGMA P2714 protease inhibitor cocktail). After a further 15 minutes, dithiothreitol (DTT) was added to a final concentration of 1 mM. The mixture was then centrifuged (23,000 g, 30 minutes, 4° C) and the supernatant collected and filtered through glass wool.

Ammonium sulfate was added to the clarified supernatant to a final concentration of 30% (176 g/L) and allowed to stir at 4°C for several hours. After stirring, the mixture was centrifuged (13,000 g, 30 minutes, 4°C) and the protein pellets collected. These pellets were dissolved in a minimum volume (~20 mL) of buffer composed of: 6 M urea, 20 mM Na-Acetate pH 5.6, 2 mM EDTA, 2 mM EGTA, 1 M NaCl, 0.5mM DTT, 0.5mM PMSF. To the solubilized pellets, 50 mg of soybean trypsin inhibitor was added. This mixture was then dialyzed twice against a buffer composed of: 6 M urea, 20 mM Na-Acetate pH 5.6, 2 mM EDTA, 2 mM EGTA, 0.5 mM DTT, 0.5 mM PMSF.

The dialysate was clarified by centrifugation (140,000 g, 40 minutes, 4°C) prior to loading it onto a pre-equilibrated with urea buffer: (6 M urea, 20 mM Na-Acetate pH 5.6, 2 mM EDTA, 2 mM EGTA, 0.5 mM DTT, 0.5 mM PMSF) CM-500 column (100 mL volume column) (figure 4 a). The column was washed with 2 – 3 column volumes of urea buffer before eluting with a linear KCl gradient (0 - 300 mM). The fractions were analyzed first by absorbance at 280 nm, and then the relevant fractions were run on a 12% SDS-PAGE gel (figure 4 b). The fractions containing the 103 kD and 79 kD polypeptides of fesselin were pooled and dialyzed against a buffer composed of: 100 mM KCl, 10 mM MOPS pH 7.2, 2 mM EDTA, 2 mM EGTA, 1 mM DTT, 0.5 mM PMSF.

The dialysate was then loaded onto a pre-equilibrated with KCl buffer (100 mM KCl, 10 mM MOPS pH 7.2, 2 mM EDTA, 2 mM EGTA, 1 mM DTT, 0.5 mM PMSF) CM-500 column (25 mL volume column). The column was washed with 2 – 3 column volumes of KCl buffer (or until absorbance reached zero) before eluting with a linear KCl gradient (100 - 300 mM). The fractions were analyzed by SDS-PAGE and western blot prior to further dialysis (figure 4 c).

The fractions containing the fesselin polypeptides were further purified using a calmodulin affinity column equilibrated with: 50 mM KCl, 20 mM Tris-HCl pH 7.4, 2 mM MgCl₂, 0.5 mM CaCl₂, 1 mM DTT. The affinity column was washed with buffer supplemented with 0.5 M KCl. After washing, the fesselin was eluted from the column with a buffer composed of: 50 mM KCl, 20 mM Tris-HCl pH 7.4, 2 mM MgCl₂, 1 mM EDTA, 1 mM EGTA, 1 mM DTT. The column was then further washed with the EDTA/EGTA buffer supplemented with 0.5 M KCl. The fractions were analyzed by SDS-PAGE before flash freezing the fractions containing fesselin (figure 4 d). This preparation yielded 5 mg of ~90% pure fesselin ranging in concentration from 0.3 mg/mL to 0.9 mg/mL. The concentrations were calculated from absorbance readings at 280 nm.

Fesselin purification method 2

The second method used for fesselin preparation was developed based on the Kolakowski (2004) method. This differed in the initial stages and in the ion exchange resin used for purification.

200 g of frozen turkey gizzards were transferred to heat seal bags and heated in a 100° C water bath for 5 – 7 minutes or until the meat browned. The gizzards were then ground in a pre-cooled meat grinder. To the ground gizzards, 1 L of ice-cold buffer was added (300 mM KCl, 50 mM MOPS pH 7.0, 0.5 mM PMSF, 0.75 mM bezamidine (0.12 g/L), 5 mg soybean trypsin inhibitor, 1 mg leupeptin, 0.5 mL Protease Inhibitor Cocktail (prepared to manufacturer specifications) (SIGMA P2714)).

The ground turkey gizzard mixture was then homogenized on ice in a Brinkmann homogenizer (model PCU7) 4 times for 10 seconds each. The mixture was then centrifuged (23,000 g, 30 minutes, 4° C) and the supernatant collected and filtered through glass wool.

Ammonium sulfate was added to the clarified supernatant to a final concentration of 30% (176 g/L) and allowed to stir at 4°C for several hours. After stirring, the mixture was centrifuged (13,000 g, 30 minutes, 4°C) and the protein pellets collected. These pellets were dissolved in a minimum volume (~20 mL) of buffer composed of: 6 M urea, 20 mM Na-Acetate pH 5.6, 2 mM EDTA, 2 mM EGTA, 1 M NaCl, 0.5mM DTT, 0.5mM PMSF.

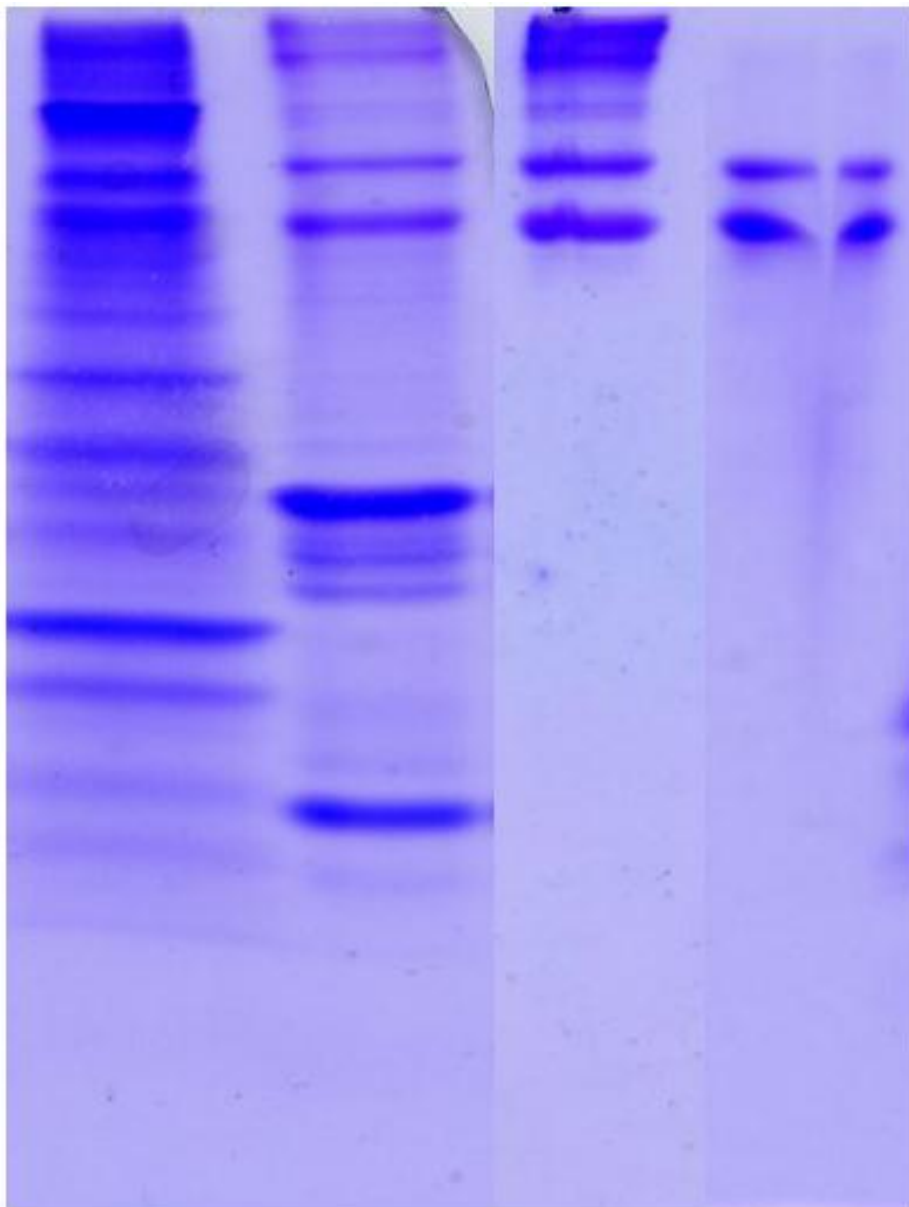
The pellets were then dialyzed twice against 1L of: 6M urea, 10 mM Tris-HCl pH 8.5, 2 mM MgCl₂, 1 mM EGTA, 1 mM DTT.

The dialysate was then clarified by centrifugation (140,000 g, 40 minutes, 4°C) before loading onto a pre-equilibrated with the same buffer as the previous dialysis SP-Sephadex column (60 mL volume column). The column was washed with 2 – 3 column volumes of the equilibration buffer supplemented with 30 mM KCl. After washing the column was eluted using a linear KCl gradient (30 - 300 mM). The fractions were analyzed first by absorbance at 280 nm, and the relevant fractions were run on a 12% SDS-PAGE gel. The fractions containing the 103 kD and 79 kD polypeptides of fesselin were pooled and dialyzed against: 50 mM KCl, 20 mM Tris-HCl pH 7.4, 2 mM MgCl₂, 1 mM DTT.

CaCl₂ was added to the dialysate to a final concentration of 0.5 mM and applied to a calmodulin affinity column pre-equilibrated with Calcium buffer (50 mM KCl, 20 mM Tris-

HCl pH 7.4, 2 mM MgCl₂, 0.5 mM CaCl₂, 1 mM DTT). The affinity column was washed with calcium buffer supplemented with 0.5 M KCl. After washing the fesselin was eluted from the column using EDTA/EGTA buffer (50 mM KCl, 20 mM Tris-HCl pH 7.4, 2 mM MgCl₂, 1 mM EDTA, 1 mM EGTA, 1 mM DTT). The column was then further washed with the EDTA/EGTA buffer supplemented with 0.5 M KCl. The fractions were analyzed by SDS-PAGE before flash freezing the fractions containing fesselin. This preparation yielded 10 mg of ~90% pure fesselin ranging in concentration from 0.5 mg/mL to 0.7 mg/mL. The concentrations were calculated from absorbance readings at 280 nm.

Both of these methods were used to purify fesselin and yield identical purity and activity of products, but the second method takes less time (3 days rather than 10) and yields more fesselin (10 mg rather than 5 mg).



103 kD
79 kD

(a)

(b)

(c)

(d)

Figure 4

Fesselin purification requires multiple steps. Because of the activity of the fesselin purifying it away from contaminants is an involved process. (a) Post ammonium sulfate precipitation. (b) Post CM-500 column I, the fesselin was identifiable but there are still several high and low molecular weight contaminants. (c) Post CM-500 column II. The higher molecular weight bands are likely aggregated fesselin considering they react to fesselin antibody (data not shown). (d) Post calmodulin affinity purification. The bands corresponding to the 103 kD and 79 kD polypeptides are free of contaminating proteins.

Smooth muscle myosin preparation

Smooth muscle myosin was prepared from frozen turkey gizzards using a modified method from Persechini (1983), and Sobieszek (1975). 150 g of turkey gizzards (chilled to near freezing) were ground twice using a pre-cooled meat grinder and suspended in 3 volumes (compared to the ground gizzards) of wash buffer (50 mM KCl, 10 mM Tris-HCl pH 7.6, 2 mM EGTA, 15 mM MgSO₄, 0.2 mM DTT, 0.1% vol Triton X-100).

The mixture was then homogenized for 3 - 5 seconds using a Brinkmann homogenizer. The pellet was recovered by centrifugation (7,500 g, 10 minutes, 4°C) and 3 more volumes of buffer were added. Homogenization and centrifugation was repeated 4 times with wash buffer and a further 4 times using wash buffer without triton X-100. After completion of the final centrifugation the pellets were homogenized in 600 mL of: 40 mM imidazole pH 7.15, 8 mM ATP, 60 mM KCl, 1 mM EDTA, 100 mg/L streptomycin, 0.5 mM DTT. The homogenization was carried out 3 times for 5 seconds. The supernatant was then collected by centrifugation (14,500 g, 20 minutes, 4°C).

After centrifugation, the supernatant was filtered through glass wool. Next 0.18 volumes of 1M MgSO₄ were added (volume calculated from volume of clarified supernatant) using a peristaltic pump at a rate of 1 mL/min. Then ATP was added to a final concentration of 2.5 mM. This mixture was allowed to sit for 10 minutes at room temperature before collecting the supernatant by centrifugation (14,500 g, 10 minutes, 4°C). The supernatant was then filtered through glass wool and centrifuged for 8 hours (40,000 g, 4° C).

The supernatant from the 8 hour centrifugation was then slowly diluted with 10 volumes of ice-cold water. The diluted crude myosin was allowed to sit for at least 2 hours at 4°C. After the myosin precipitated in the water, the pellet was recovered by centrifugation (14,500 g, 15 minutes, 4°C). The protein containing pellet was then suspended in 1 volume of water with a glass/Teflon homogenizer (volumes based on the pellet). Next at 4°C 0.0038 volumes of 100 mM EGTA were added. Then 0.05 volumes of Na₂HPO₄, pH 7.6 were added. Then 0.25 volumes of 1 M MgSO₄ were added. Finally 0.063 volumes of 100 mM ATP were added. All of these additions were done slowly using a peristaltic pump (0.5 mL/min).

The mixture was then allowed to stand for 10 minutes at 4°C. The supernatant was then separated and collected using centrifugation (150,000 g, 2 hours, 4° C). The supernatant was then diluted with 10 volumes of ice-cold water. The myosin precipitate was then collected by centrifugation (23,000 g, 15 minutes, 4° C). The collected myosin pellets were dissolved in a minimum volume of: 0.3 M KCl, 10 mM Tris-HCl pH 7.6, and 0.2 mM DTT.

To further purify the myosin it was loaded onto a Sepharose 4B column that was equilibrated with a buffer composed of: 0.3 M KCl, 10 mM Tris-HCl pH 7.6, and 0.2 mM DTT. Prior to loading onto the column the myosin was diluted to 3.5 mg/mL. To prevent phosphorylation of the myosin light chains 0.5 mM EGTA was added to the buffer. This preparation yielded 0.5 - 1 g of purified myosin which could be used immediately or safely stored at -20° C after addition of glycerol to 50% v.

Actin preparation

Actin was purified from acetone powders generated from rabbit erector spinae muscle. This method is based on Ebashi (1965). 9 grams of acetone powder were added to 270 mL of Extraction buffer (0.5 mM ATP, 2 mM Tris-HCl pH 7.8, 0.1 mM CaCl_2 , 1 mM β -mercaptoethanol) extraction was carried out on ice. The actin was gently stirred once every 10 min for a total of 30 min as to reduce the extraction of contaminating proteins such as α -actinin or tropomyosin.

The supernatant was then collected by centrifugation (47,000 g, 45 minutes, 4°C) and filtered through glass wool. Solid KCl was then added to the supernatant to a final concentration of 3.3 M. The KCl addition was carried out at room temperature with stirring until the solution reaches 15°C. The solution was then cooled to 5°C.

The supernatant was then clarified by centrifugation (47,000 g, 45 minutes, 4°C). The supernatant was then dialyzed against 32 volumes of: 2 mM Tris-HCl pH 7.6, 1 mM MgCl_2 .

After dialysis 4 M KCl was added to the dialysate to give a final concentration of 0.8 M. This was allowed to stir at 4°C for 1 hour. The pellets were then collected using centrifugation (147,000 g, 90 minutes, 4°C), dissolved in 25 mL of the extraction buffer then homogenized with a glass/Teflon homogenizer. The resuspended pellets were then dialyzed against 2 exchanges of at least 20 volumes of extraction buffer.

The actin was then placed in a beaker and stirred while adding imidazole to 10 mM and MgCl_2 to 1 mM. The solution was then dialyzed at 4°C against 2 exchanges of 20 volumes of: 4 mM imidazole pH 7.0, 2 mM MgCl_2 , 0.5 mM ATP. To store the actin at 4°C NaN_3 was added to 0.01% directly to the actin. This preparation yielded 100-180 mg of actin.

Myosin and Calmodulin Affinity columns

Affinity columns were prepared from lyophilized CNBr-activated sepharose-4B resin according to manufacturer's instructions (GE Healthcare 71-7086-00 AF). The resin was weighed out according to the manufacturers specifications (1g = ~3.5 mL) for the myosin subfragment columns between 0.5 – 2 mL final volume of resin was used.

Prior to the preparation of the resin, the desired ligand was dialyzed into the coupling buffer (0.5 M NaCl .1 M NaHCO₃ pH 8.4) which facilitates the CNBr reaction and subsequent covalent bonding of the protein to the sepharose beads. The amount of ligand was added at 5 mg/mL of swollen resin.

The weighed out dry resin was washed and allowed to swell in 1 mM HCl. This swelling and washing was critical to wash away stabilizing compounds in the resin and prepare it for coupling. After the resin swelled for 15 minutes it was further rinsed with 1 mM HCl (200 mL/g of dry resin) and then 2 column volumes of milli-Q water.

The resin was immediately mixed with the ligand in a vial with adequate volume for inversion mixing using a rocking mixer to avoid damaging the protein or the sepharose beads. For the calmodulin affinity columns mixing, was at room temperature for 1 hr. For the myosin and myosin-subfragment columns, mixing was at 4°C for 16 hours. The buffer was decanted and the remaining CNBr activated beads were blocked with 1 M ethanolamine pH 8.0. The ethanolamine was added directly to the resin and allowed to block for 1 hour at room temperature for calmodulin columns or for 16 hrs at 4°C for the Myosin and Myosin subfragment columns.

The resin was transferred to a column and rinsed with 2 column volumes of coupling buffer. To remove any unreacted calmodulin. The calmodulin resin was rinsed with coupling buffer (0.5 M NaCl, 0.1 M NaHCO₃, pH 8.4), followed by acetate buffer (0.5 M NaCl, 0.1 M Na-Acetate, pH 4.0). For the myosin and myosin subfragments, the columns were rinsed with only coupling buffer in a far greater volume (10 column volumes minimum).

To determine the efficiency of coupling, a small sample of resin was tested using a Bradford colorimetric assay. This was controlled using resin reacted with ethanolamine alone and the eluted protein from the reaction as well as other protein standards.

Fluorescent labeled proteins

For several of the studies presented here, fluorescently labeled proteins were utilized. All of the reagents used involved an iodoacetamide conjugation to covalently link the fluorophore to a cysteine residue on the target protein.

IANBD fesselin

Turkey gizzard fesselin was labeled with N,N'-Dimethyl-N-(Iodoacetyl)-N'-(7-Nitrobenz-2-Oxa-1,3-Diazol-4-yl)Ethylenediamine (IANBD) using a 5 fold molar excess for 12 hours at 4°C.

The fesselin was first reduced by adding DTT to a concentration of 2 mM then dialyzing the fesselin against 3 exchanges of 100 volumes of: 85 mM NaCl, 15 mM Na₂HPO₄ pH 7.0. The IANBD was prepared at a stock concentration of 10 mg/mL in

dimethylformamide (DMF). The IANBD was added at 5 - fold molar excess to the fesselin with very rapid mixing. The mixing was required to minimize the damage that the DMF did to the fesselin. After mixing the probe with the fesselin, the vial was covered and light protected.

This reaction was allowed to sit at 4°C for 12 hours. After 12 hours DTT was added to 2 mM final concentration to quench the reaction. The unreacted probe was removed by centrifugation (120,000 g, 40 minutes, 4°C). The extent of labeling was determined using a UV-Vis spectrophotometer scanning from 600 to 250 nm. Labeled IANBD absorbs at 492 nm, the extinction coefficient for IANBD in water is $21,000 \text{ cm}^{-1} \text{ M}^{-1}$. For fesselin an extinction coefficient of 1 at 280 nm was used for initial estimation of concentration, and a Bradford or Lowry assay was used for a further determination.

Under the conditions presented here, the extent of labeling was on average of 5:1 label : protein.

Acrylodan tropomyosin

Tropomyosin was reduced prior to labeling in a buffer of: 100 mM KCl, 10 mM Na_2HPO_4 (pH 6.5), 5 mM EDTA, 1 mM dithiothreitol (DTT). After dialysis additional Na_2HPO_4 was added to bring concentration up to 50 mM and DTT was added to a final concentration of 10 mM. After this addition the tropomyosin was allowed to incubate at 37°C for 30 minutes.

Post incubation the tropomyosin was dialyzed twice against 500 mL of: 3 mM MOPS pH 7.5, 0.1 mM EDTA. Guanidine HCl was added to a final concentration of 4 M. a 5-fold molar excess of 6-Acryloyl-2-Dimethylaminonaphthalene (acrylodan) was

added and allowed to react for 8 hrs at room temperature, in the dark under a nitrogen atmosphere. Adding excess DTT was used to quench the reaction.

The unreacted probe was removed by centrifugation (120,000, 20 minutes, 4°C) and the supernatant was retained. Post centrifugation, the supernatant was dialyzed against 20 volumes of 4 M guanidine HCl, 3 mM MOPS pH 7.5, 0.1 mM EDTA.

Tropomyosin was further dialyzed twice against 15 volumes of 40 mM NaCl, 5 mM MOPS pH 7.5, 0.2 mM EDTA, 0.01% NaN₃. The extent of labeling was then determined using a UV/vis spectrophotometer scanning from 600 to 250 nm. The determination used the extinction coefficient for acrylodan at 372 nm of 14,400 cm⁻¹, M⁻¹ and an extinction coefficient of 0.75 ε^{0.1%} at 280 nm for tropomyosin. The labeling efficiency for this preparation was 70 – 80% 1 label : 1 tropomyosin.

Pyrene actin

Pyrenyl-iodoacetamide labeled actin was prepared from f-actin in actin buffer: 4 mM imidazole pH 7.0, 2 mM MgCl₂. Actin was diluted to 2 mg/mL, dilution buffer (100 mM Tris pH 8.0, 1 M KCl, 20 mM MgCl₂, 1 mM CaCl₂, 0.1% NaN₃) accounted for 10% of the final volume (e.g. 20 mg actin, 1 mL dilution buffer, 9 mL H₂O) and stirred until a homogeneous mixture.

Pyrenyl-iodoacetamide (pyrene) was prepared at a concentration of 14 mg/mL in DMF. The pyrene solution was then added to the actin in the dark and allowed to incubate for 12 hrs at 4°C. DTT was added to quench the reaction.

The actin was then centrifuged to remove unreacted pyrene (140,000 g, 20 min, 4°C). F-actin was then recovered by centrifugation (145,000 g, 1 hr, 4°C). The pellets

contained the pyrene-labeled actin; these were homogenized and dialyzed against 500 mL of actin buffer. The extent of labeling was then determined using a UV/vis spectrophotometer scanning from 600 to 250 nm. The determination used the extinction coefficient for pyrene at 344 nm of $22,000 \text{ cm}^{-1}, \text{ M}^{-1}$ and a lowry assay for the actin. The labeling efficiency for this preparation was 80% 1 pyrene : 1 actin.

Protein cross-linking

The crosslinking reaction buffer used was: 85 mM NaCl, 15 mM Na_2HPO_4 pH 7.4. This same buffer composition was used for all the cross-linking reagents For the primary amine reactive reagents Tris buffer was added to quench unreacted cross-linker. To quench the cysteine reactive reagents, DTT was added.

For non-UV activated cross-linkers, the incubation time varied slightly. 3,3'-dithiobis(sulfosuccinimidylpropionate) and dimethyl 3,3'-dithiopropionimidate dihydrochloride were both allowed to react for a total of 30 minutes at room temperature (25°C), the reagents were allowed to react with fesselin alone for 2 minutes before myosin was added. After the 30 minute reaction time the remaining unreacted cross-linker was quenched with 10% v 250 mM Tris buffer.

The N,N'-1,4-Phenylene-dimaleimide (PPDM) was allowed to react in a similar way to the amine-to-amine cross-linkers. The PPDM was allowed to react for a total of 30 minutes at room temperature (25°C), with fesselin alone for 2 minutes before myosin was added. After the 30 minute reaction time the remaining unreacted cross-linker was quenched with 10% v 20 mM DTT.

The UV light activated cross-linking reagents were incubated with fesselin for 30 minutes at room temperature in light protected vessels. After 30 minutes myosin was added to the reaction, and allowed to incubate further for 20 minutes at 37°C. After 20 minutes the reaction was exposed to UV light for 30 seconds using an Oriel high voltage UV light source to activate the cross-linker.

With each of the reactions control experiments were performed using myosin alone and fesselin alone. A sample from each experiment was then run on a 5% SDS-PAGE and stained with Coomassie blue. A sample was also taken and ran on an agarose/acrylamide gel with an acrylamide percentage of 3%. This was required to observe the large complexes formed when myosin was cross-linked.

Protein co-sedimentation

For the sedimentation assays, smooth muscle myosin was dialyzed into a buffer composed of: 500 mM NaCl, 10 mM MOPS pH 7.0, 2 mM MgCl₂, 1 mM DTT. The fesselin used was dialyzed into the experimental buffer: 94 mM NaCl, 10 mM MOPS pH 7.0, 2 mM MgCl₂, 1 mM DTT. The final buffer concentration for each experiment was adjusted to: 94 mM NaCl, 10 mM MOPS pH 7.0, 2 mM MgCl₂, 1 mM DTT. The proteins were mixed (1:1 molar ratio fesselin: myosin) in the centrifuge tubes and allowed to stand for 5 minutes before centrifugation (13,000 g, 7 minutes, 4°C). The supernatants and pellets were then separated and analyzed by 12% SDS-PAGE. This same operation was completed for the fesselin peptides, but analyzed using 15% SDS-PAGE at 19:1 acrylamide: bis-acrylamide.

Transient kinetics

The rate of dissociation of myosin from actin following rapid mixing with ATP was measured by light scattering on a SF20 sequential mixing stopped-flow spectrometer (Applied Photophysics Ltd., Leatherhead, Surrey, United Kingdom). The temperature was controlled with a circulating water bath at 10° C. The excitation wavelength was set using a monochromator using slit widths of either 0.5 or 1 mm.

Emission wavelengths were selected with high-pass filters. Acrylodan fluorescence was measured with excitation at 391 nm with emission regulated by a Schott (Duryea, PA) GG 455 high-pass filter with a 455 nm midpoint. (2'(3')-O-(*N*-methylanthraniloyl)-ATP) MANT fluorescence changes were monitored via excitation at 366 nm and emission measured with an Oriel model 51270 high-pass filter. Pyrene fluorescence was measured with an excitation of 366 and emission measured with an Oriel model 51270 high-pass filter. Fluorescein fluorescence was measured with an excitation of 490 and emission measured with an Oriel model 51294 high-pass filter. IANBD fluorescence was measured with an excitation of 490 and emission measured with an Oriel model 51294 high-pass filter (Table 1). Light scattering measurements were taken by increasing the emission wavelength above the working range of the excitation filter (600nm for the 455 nm high-pass filter).

Probe	λ_x	λ_m	$\lambda_s/\lambda_c/\lambda_{p1}$	Source
Pyrene	344	386, 397	340/385/480	Oriel 51270
Acrylodan	391	500	390/455/530	Oriel 51284
IANBD	492	536	440/515/580	Oriel 51294
MANT-ATP	366	448	340/385/480	Oriel 51270
Fluorescein	490	515	440/515/580	Oriel 51294

Table 1

Fluorescent probes used. The probe names are the common names for each of the probes and the filters are all high-pass filters with the Oriel numbers given. λ_s is the stop band limit. λ_c is the midpoint of the filter (50% transmittance). λ_{p1} is the passband limit or the wavelength of maximum transmittance.

The state of unphosphorylated smooth muscle myosin

To determine the conformational state of the unphosphorylated smooth myosin under the experimental conditions used in these studies, we examined the rates of product release by myosin (ADP + Pi). This was accomplished through monitoring MANT-ATP fluorescence on a sequential mixing stopped-flow. MANT-ATP was synthesized as described by Hiratsuka (1983). The smooth myosin was mixed with MANT-ATP and allowed to react long enough (100 ms) for the ATP to bind and equilibrium to be reached between the MANT-ATP and MANT-ADP-Pi states. The MANT-ATP-myosin was then rapidly mixed with 100-fold excess of unlabeled ATP to displace the MANT-ATP and MANT-ADP-Pi (giving a decline in fluorescence). This gave a monoexponential decay curve with a rate of 0.66 s^{-1} for 500 mM KCl buffer, this was consistent with previously published values for stabilized 6S myosin at 600 mM KCl (Cross 1998 , Suzuki 1985). The procedure was repeated under the conditions used for the experiments (94 mM NaCl). The decay under these conditions fit to a biexponential with a k_1 of 0.6 s^{-1} and k_2 of 0.036 s^{-1} . This measurement was consistent with equilibrium between the active 6S conformation of myosin and the inactive 10S conformation (figure 5). From these experiments it was clear that the myosin used within these studies was operating, as unphosphorylated myosin should under the experimental conditions.

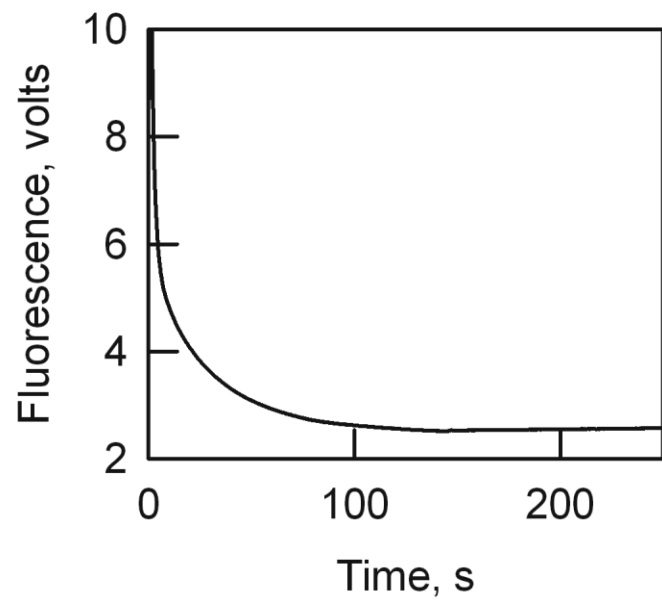


Figure 5

MANT-ATP measurements show that the myosin used was regulated properly for unphosphorylated smooth myosin. This transient was collected using sequential mixing stopped-flow. First 0.05 μM smooth myosin was mixed with equimolar MANT-ATP. After 0.1 seconds this was mixed with 100 fold molar excess of unlabeled ATP. The transient shows MANT fluorescence as a function of time as products (MANT-ATP, MANT-ADP) detach from myosin $k_1 = 0.6 \text{ s}^{-1}$, and $k_2 = 0.036 \text{ s}^{-1}$. Conditions: 94 mM NaCl, 10 mM MOPS pH 7.0, 2 mM MgCl_2 , 1 mM dithiothreitol, 10°C (Reprinted with permission from Kingsbury et al. copyright 2013 American Chemical Society)

Electron microscopy

Negative staining electron microscopy was used to visualize myosin and actin filaments. The technique used was modified from J. Robin Harris (2007). Carbon-coated Formvar nickel grids (200 mesh) were negatively charged using an EMS 100 Glow Discharge unit immediately prior to applying protein solutions. Solutions of myosin, actin, and fesselin were prepared by adding concentrated stocks to a buffer composed of: 94 mM NaCl, 10 mM MOPS pH 7.0, 2 mM MgCl₂, and 0.1 mM DTT.

Proteins were first mixed at the requisite concentrations for the experiments on a piece of Parafilm before application to the grids. The proteins were allowed to incubate on the grids for 30 seconds in all cases.

ATP grids

For the experiments involving ATP the preparation of the grids required a specific rinse to reduce ATP-stain reactions. After the 30 second incubation with the protein the solution was removed by touching a piece of Whatman #1 filter paper. The grid was then rinsed with 50 µL of 0.1 M NH₄-Acetate (pH 7.0). The rinse buffer was then removed with Whatman #1 filter paper to the edge of the grid.

The ammonium acetate rinse was required to eliminate precipitation of uranyl phosphate from the stain (Matijević 1958).

The rinsed grids were then stained with 1% aqueous uranyl acetate. Whatman #1 filter paper was placed in contact with the edge of the grid while 10 µL of 1% uranyl acetate was applied to the grid. After the initial stain, a further 10 µL of uranyl acetate

was applied to the grid surface. The stain was allowed to incubate for 45 seconds before removal with filter paper. The grids were air dried prior to analysis.

ATP-free grids

After the 30 second incubation with the protein the solution was removed by touching a piece of Whatman #1 filter paper to the edge of the grid. The grid was then rinsed with 50 μ L of the protein buffer. The buffer rinse was then removed with Whatman #1 filter paper.

The rinsed grids were then stained with 1% aqueous uranyl acetate. Whatman #1 filter paper was placed in contact with the edge of the grid while 10 μ L of 1% uranyl acetate was applied to the grid. After the initial stain, a further 10 μ L of uranyl acetate was applied to the grid surface. The stain was allowed to incubate for 45 seconds before removal with filter paper. The grids were air dried prior to analysis.

Grid visualization

After application of sample and staining, the grids were visualized in a JEOL 1200EX transmission electron microscope at an accelerating voltage of 80 kV. Images were recorded using a SIS ImageView III CCD camera (Olympus, Tokyo, Japan). Examples of the resultant images can be seen throughout this thesis as well as in figure 6 A and B. Figure 6 C and D shows a representation of how the electron beam interacts with negative and positive stained samples.

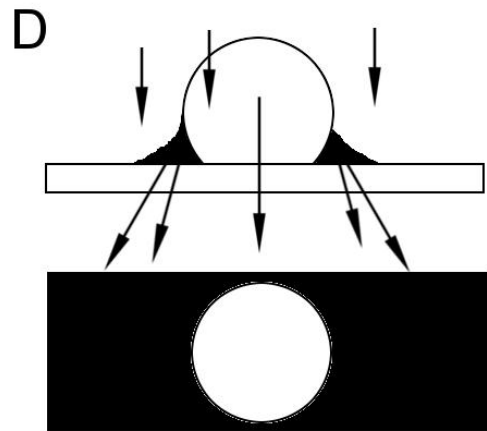
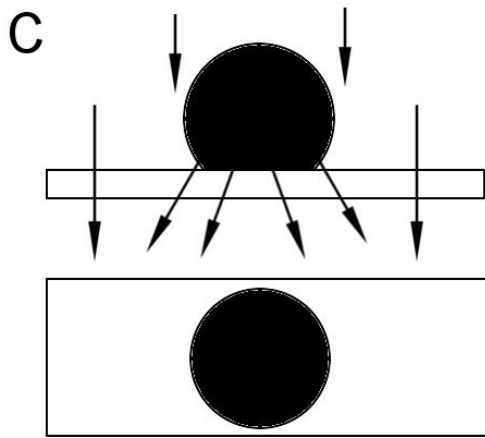
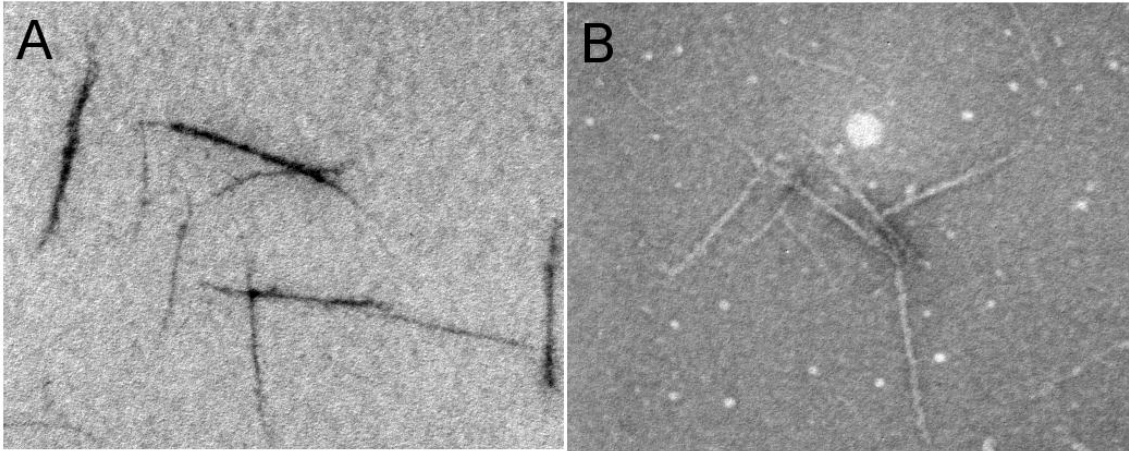


Figure 6

The use of negative and positive stain electron microscopy gave different information for the same samples. A) Positive stained myosin filaments. Samples stained in this manner were used to measure some aspects of myosin filaments. These samples lacked some detail compared to negatively stained samples but gave accurate measurements. B) Negative stained myosin filaments. This was the major sample type used for the experiments. Negative staining gives more detail than positive stain in most cases, and allows for observation of more complex structures. C) Schematic of how positive stained objects interact with an electron beam. The electrons are directly absorbed or reflected off the sample itself. This schematic shows both a side view and a top down view. D) Schematic of negatively stained object. The heavy metal stain pools around the object and interacts with the electron beam. This gives the outline of details on the sample.

Results

The initial studies with fesselin focused on the interactions between fesselin and actin. It was later found that fesselin also binds to myosin. That finding initiated the questions that led to the present research. Knowing that fesselin bound to both actin and to myosin led to the question of whether fesselin can crosslink myosin and actin together under relaxed conditions. That is, could a function of fesselin be to organize actin and myosin in a contractile competent manner? We subsequently investigated the ability of fesselin to stabilize myosin filaments to determine if fesselin organized all components of the contractile unit.

Part I. The interactions of fesselin with actin-myosin and myosin

Fesselin reduces the rate of dissociation of myosin and actin by ATP.

Fesselin promotes actin polymerization and actin bundle formation; these activities suggest that fesselin helps to organize the contractile apparatus. Fesselin also binds to myosin. That raised the possibility that fesselin can tether actin and myosin filaments to promote organization of a contractile unit. Another protein studied in our laboratory, caldesmon, binds to actin (Hemric & Chalovich 1988) and to myosin

(Katayama et al. 1995) and does form reversible crosslinks between myosin and actin (Marston et al. 1992, Chalovich et al. 1997). We studied the effect of fesselin on the dissociation of myosin from actin following the rapid addition of ATP.

Myosin binds very tightly to actin in the absence of ATP. Upon the addition of ATP to actin-myosin the complex rapidly dissociates. This creates a challenge for cells because myosin needs to be in proximity to actin to permit contraction to occur and yet, cells have sufficient ATP to weaken the attachment of myosin to actin.

My work started by looking at the effects of various concentrations of fesselin on the dissociation of actin and myosin using light scattering changes in rapid kinetics stopped-flow. Light scattering voltage changes monitor changes in particle size. Actin-myosin complexes were mixed rapidly with ATP in the absence of fesselin (figure 7, curve 1). The rapid decrease in voltage in figure 7 shows the dissociation of myosin from actin caused by ATP binding. Fesselin greatly reduced the amount of filament dissociation on this time scale. The actin-myosin curve (curve1) was biphasic with two apparent rate constants: $k_1 = 4.2 \text{ s}^{-1}$ and $k_2 = 0.24 \text{ s}^{-1}$. Addition of $0.05 \text{ }\mu\text{M}$ fesselin (curve 4) reduced the observed rate constants to 1.6 s^{-1} and 0.16 s^{-1} , respectively, or nearly 40% of their original values. Fesselin also reduced the amplitude, indicating the possibility that multiple populations of actin- fesselin- myosin filaments exist: one that dissociated at a rate that was around 40% of the rate of actin- myosin filaments and another population that did not disassemble on the experimental time scale.

Because the process being observed in the stopped-flow was the dissociation of large filaments it was possible to observe the initial and final states of the process by

electron microscopy. We therefore enlisted the help of Dr. Randall Renegar to understand more clearly what we are observing by rapid kinetics.

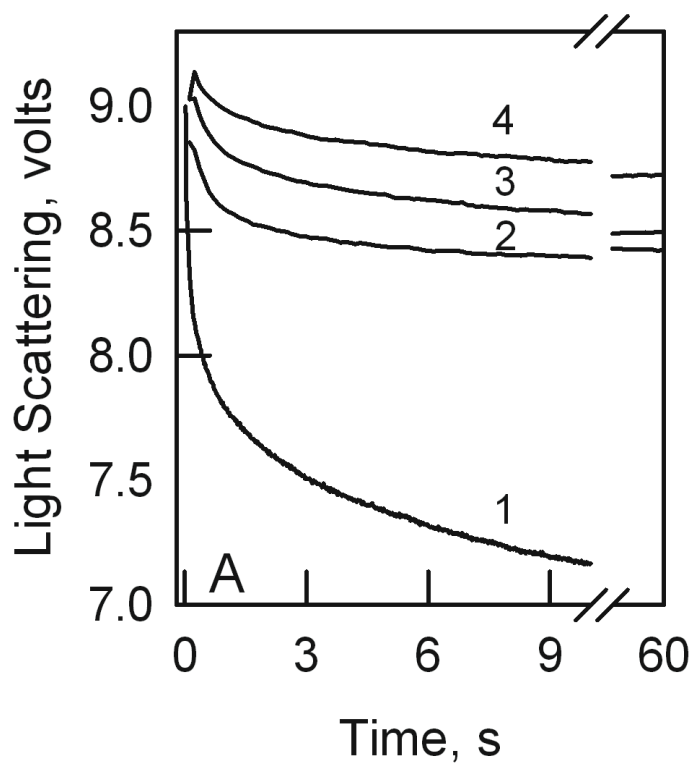


Figure 7

Fesselin increased the resistance of actin-myosin filaments against ATP induced dissociation. Light scattering transients for 0.2 μM phalloidin-actin with 0.05 μM smooth myosin with varying fesselin concentrations were collected. All these transients used 2 mM ATP final. 1) 0.0 μM fesselin, $k_1 = 4.2 \text{ s}^{-1}$ and $k_2 = 0.24 \text{ s}^{-1}$. 2) 0.0125 μM fesselin, $k_1 = 2.3 \text{ s}^{-1}$ and $k_2 = 0.23 \text{ s}^{-1}$. 3) 0.025 μM fesselin, $k_1 = 1.7 \text{ s}^{-1}$ and $k_2 = 0.13 \text{ s}^{-1}$. 4) 0.05 μM fesselin, $k_1 = 1.6 \text{ s}^{-1}$ and $k_2 = 0.16 \text{ s}^{-1}$. The reduced amplitude of the transients with fesselin suggests that most actin–fesselin–myosin complexes were stable on this time scale. Conditions: 94 mM NaCl, 10 mM MOPS pH 7.0, 2 mM MgCl_2 , 1 mM dithiothreitol, 10°C (Reprinted with permission from Kingsbury et al. copyright 2013 American Chemical Society)

Electron microscopy shows fesselin stabilizing actin and myosin against ATP induced dissociation

To confirm the results of the stopped-flow experiments as well as to visualize the formation and stabilization of the actin– myosin complex in the presence or absence of fesselin, negative staining of filaments and examination using the electron microscope was performed. Figure 8 A shows the absence of myosin filaments on grids containing actin, myosin and ATP. The addition of fesselin figure 8 B stabilized the myosin filaments . This observation indicates that fesselin stabilizes myosin filaments, in the presence of ATP, and keeps those myosin filaments in close proximity to actin filaments. The images used for figure 8 are representative of the random fields taken from the grids. In addition to random fields, the grids were further analyzed to confirm the absence of myosin filaments when fesselin was not present. The same concentration of ATP was used for these experiments as in the rapid-kinetics (2 mM).

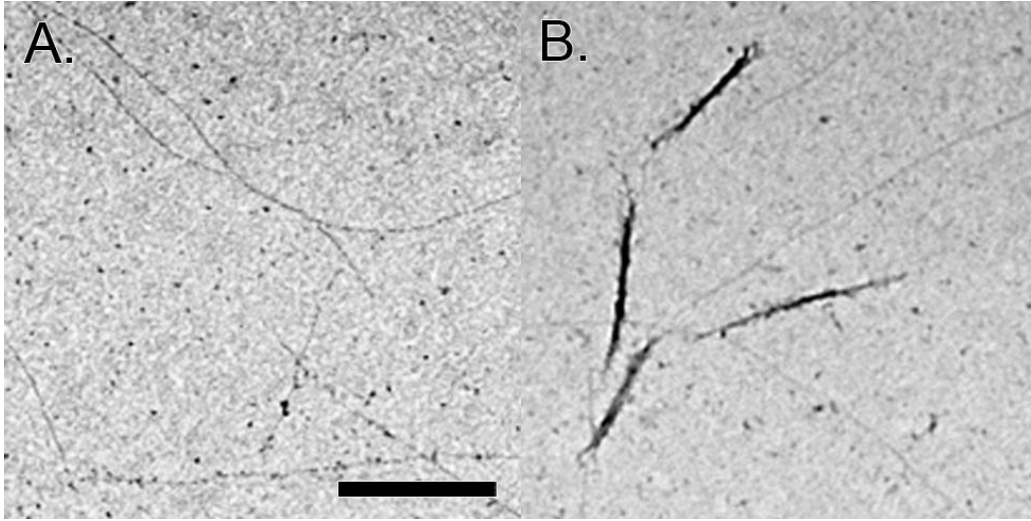


Figure 8

Electron microscopy images showing myosin filaments binding along actin filaments in the presence of ATP only when fesselin is present. Smooth muscle myosin and actin with or without fesselin were added to the grid in the presence of ATP: (A) actin–myosin complex with ATP and (B) actin–myosin–fesselin complex with ATP. Actin (0.2 μM) was used with 0.05 μM myosin and 0.1 μM fesselin. Conditions: 94 mM NaCl, 10 mM MOPS pH 7.0, 2 mM MgCl_2 , 1 mM dithiothreitol, 10°C (Reprinted with permission from Kingsbury et al. copyright 2013 American Chemical Society)

Fesselin stabilizes actin-myosin by tethering both proteins together and not by reducing the detachment rate from the specific actin-myosin interface.

The stabilization of the actin-myosin complex by fesselin could occur because fesselin (i) reduces the rate of ATP binding to myosin, (ii) reduces the rate of detachment of actin from the specific binding site on myosin, or (iii) tethers actin and myosin without a direct effect on the specific actin-myosin binding site.

To determine if fesselin was having an effect on the detachment rate of myosin from actin or the rate of ATP binding to myosin, experiments were performed with heavy meromyosin (HMM). HMM constitutes a portion of myosin that includes the ATP binding pocket, the actin binding domain, as well as the portion of the neck linker that holds the two heads of myosin together, HMM lacks a large portion of the coiled-coil tail of myosin (figure 9). The experiments performed with HMM were similar to those done with intact myosin. HMM and actin were mixed rapidly with 4 mM ATP in a stopped-flow spectrometer and the changes in light scattering were monitored. These studies showed that fesselin had a minimal effect on dissociation of HMM from actin (figure 10). A single-exponential process with a rate constant of 320 s^{-1} was observed without fesselin (curve 1). Addition of $0.05 \text{ }\mu\text{M}$ fesselin reduced the rate constant to 230 s^{-1} (curve 2), while the rate constant was 280 s^{-1} (curve 3) in the presence of $0.2 \text{ }\mu\text{M}$ fesselin. These data suggest that fesselin tethers actin and myosin together and that this tethering likely occurs between a binding of fesselin to the light meromyosin portion of myosin (LMM).

LMM	HMM
Rod	S-1

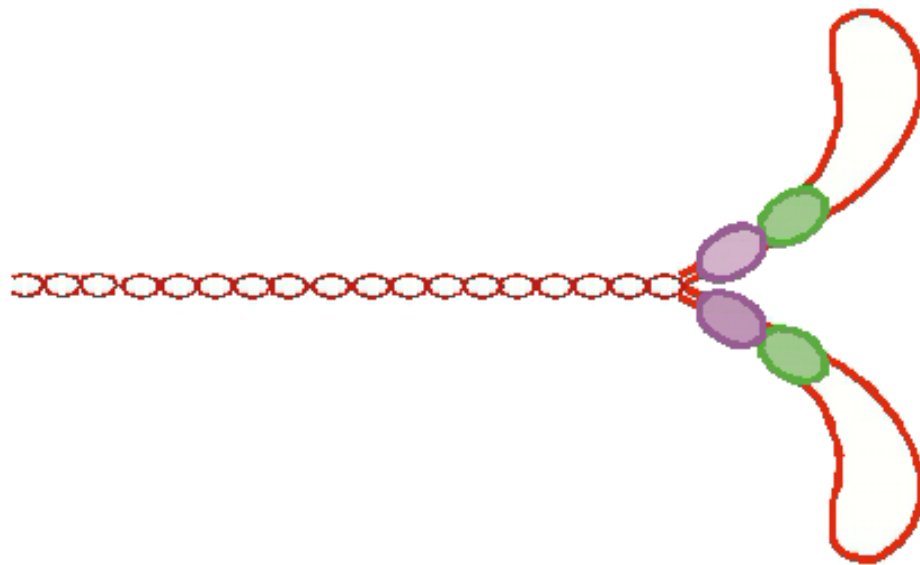


Figure 9

Myosin can be digested with proteases into several fragments with differing functions. The two main fragments that have actin binding activity and ATPase activity are heavy meromyosin (HMM), and myosin subfragment-1 (S-1). In addition to these there is also myosin Rod that is composed of the entire coiled-coil domain, and light meromyosin (LMM), which is the rear portion of the Rod.

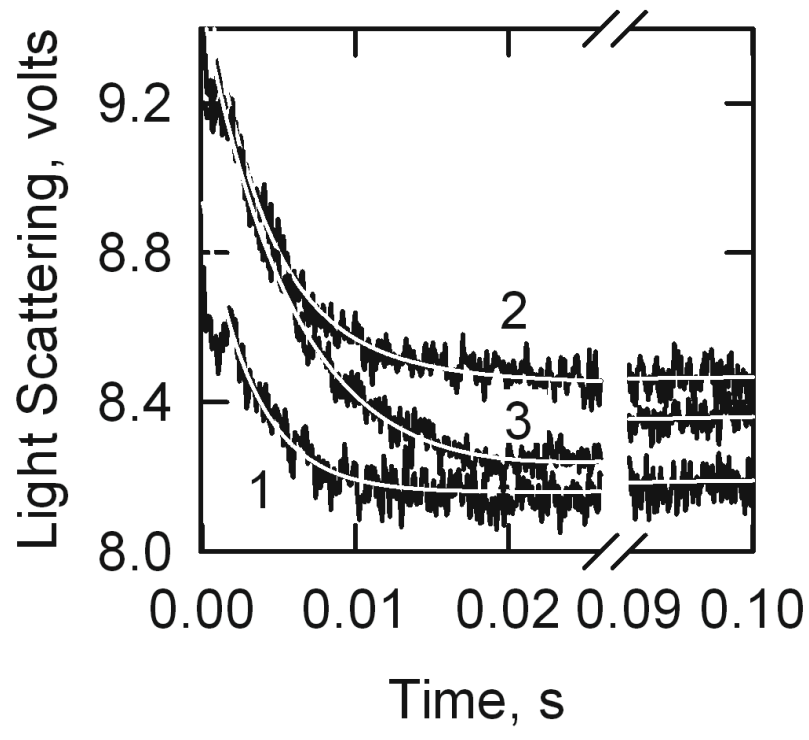


Figure 10

Fesselin had only slight effects on HMM dissociation from actin. Light scattering transients for 0.2 μM phalloidin-actin with 0.05 μM smooth heavy meromyosin (HMM) with varying fesselin concentrations were collected. All these transients used 2 mM ATP final. 1) 0.0 μM fesselin, $k_1 = 320 \text{ s}^{-1}$. 2) 0.05 μM fesselin, $k_1 = 230 \text{ s}^{-1}$. 3) 0.2 μM fesselin, $k_1 = 280 \text{ s}^{-1}$. Conditions: 94 mM NaCl, 10 mM MOPS pH 7.0, 2 mM MgCl_2 , 1 mM dithiothreitol, 10°C (Reprinted with permission from Kingsbury et al. copyright 2013 American Chemical Society)

To further examine the possibility of the tethering model of fesselin's interaction with the actin-myosin complex pyrene-labeled actin was used. Pyrene-actin fluorescence has been used to monitor specific myosin binding (Geeves & Lehrer 1994, Crosbie et al. 1991, Franklin et al. 2012). We designed experiments that were similar to the light scattering studies presented earlier but, using pyrene-actin fluorescence to measure the rate of the myosin-actin bond breaking. A complex of myosin and pyrene actin was rapidly mixed within the stopped-flow with ATP (2 mM final concentration), the fluorescence change that occurs correlates with the myosin-actin bond breaking.

Figure 11 shows that the binding curves are biphasic in agreement with the model suggested by Trybus & Taylor (1980) and McKillop & Geeves (1991): $M + A = M-A = MA^*$. Fluorescence measurements measure the initial collision event while pyrene fluorescence measures the subsequent isomerization. The interesting result is that fesselin has very little effect on the pyrene fluorescence rate constant. That is, fesselin has little direct effect on actin-myosin bond breaking. The results of the pyrene experiments lend more evidence to the tethering model of the fesselin interaction.

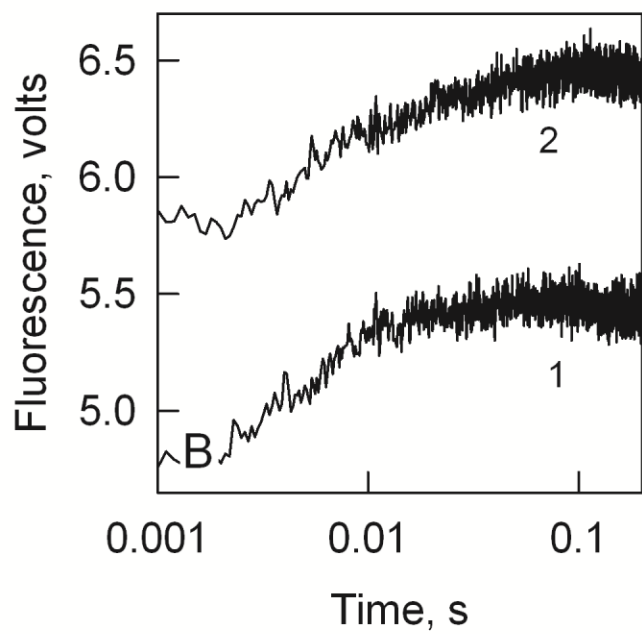
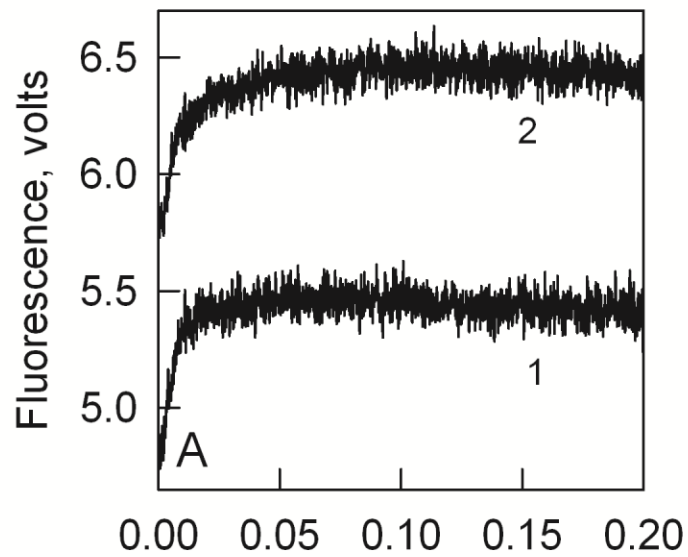


Figure 11

Fluorescence transients for 0.2 μM phalloidin-pyrene-actin with 0.05 μM smooth myosin with and without fesselin. These experiments used 2 mM ATP final. A) Linear time scale shows that the majority of change is very rapid, 1) 0.0 μM fesselin 2) 0.05 μM fesselin. B) Logarithmic time scale better displays the small differences between 1 and 2. 1) 0.0 μM fesselin 2) 0.05 μM fesselin. Conditions: 94 mM NaCl, 10 mM MOPS pH 7.0, 2 mM MgCl_2 , 1 mM dithiothreitol, 10°C.

The next set of experiments utilized fluorescein labeled myosin to monitor the rates of ATP binding to myosin. A complex of actin and fluorescein-myosin mixture was rapidly mixed within the stopped-flow with ATP.

The experiments with fluorescein-myosin were unable to show any further evidence for how fesselin interacts with actin and myosin because the fluorescence changes only monitored ATP binding. The transients collected were identical with and without actin present (figure 12). The fluorescence changes induced by ATP binding are indistinguishable from each other because actin accelerates ATP-hydrolysis and product release steps of the myosin cross-bridge cycle, not the ATP binding step directly. To provide evidence for how fesselin interacts with actin and myosin a different approach was required. The required method would be one that reported the rate of myosin detachment without reporting the effects of fesselin and actin.

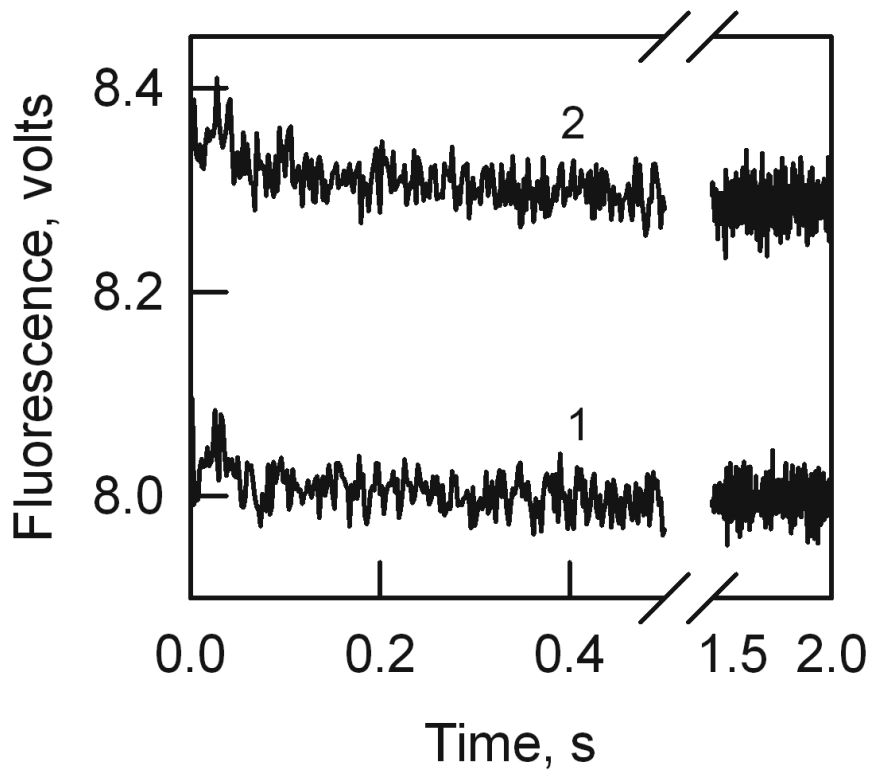


Figure 12

Fluorescein-smooth myosin measurements were unable to monitor actin-myosin dissociation. The changes in fluorescence with fluorescein monitored ATP binding to myosin which showed no changes with or without actin / fesselin. Fluorescence transients were collected with and without actin. These experiments used 2 mM ATP final. 1) 0.0 μ M phalloidin-actin 2) 0.2 μ M phalloidin-actin. Conditions: 94 mM NaCl, 10 mM MOPS pH 7.0, 2 mM $MgCl_2$, 1 mM dithiothreitol, 10°C

The next set of experiments attempted to definitively prove that fesselin tethers actin and myosin together. This was accomplished by adding acrylodan labeled tropomyosin to the system. Tropomyosin is an actin binding protein that spans seven actin protomers, and changes position when myosin binds or detaches. In the case of acrylodan labeled tropomyosin, this change in position results in a change in fluorescence (Chalovich et al. 2011, Franklin et al. 2012, Borrego-Diaz & Chalovich 2010). Experiments were first performed with unlabeled tropomyosin to determine if the addition of tropomyosin severely impacted the rate of dissociation of myosin from actin. It was found not to significantly impact the dissociation (data not shown). With this in mind the experiments were then performed in the same way as the light scattering experiments (figure 7) but with the addition of acrylodan-tropomyosin.

The light scattering decrease was similar to that in figure 7. The light scattering changes over fesselin concentration it is plotted in figure 13 B as open circles (\circ) the rates were also plotted as a function of fesselin concentration for the acrylodan fluorescence in figure 13 B as open squares (\square). Figure 13 A shows a comparison of the acrylodan fluorescence for the ATP induced breakup of the actin-tropomyosin-myosin complex in the presence and absence of fesselin. The apparent rate constants were 1.6 s^{-1} and 0.17 s^{-1} without fesselin and 1.4 s^{-1} and 0.15 s^{-1} with $0.25 \mu\text{M}$ fesselin. This is a very minimal decrease in fluorescence when compared to the changes in rate measured by light scattering.

Figure 13 B shows the dependencies of light scattering and acrylodan tropomyosin fluorescence on fesselin concentration. Fesselin had a large effect on the light scattering reducing it from 2.8 s^{-1} to 0.5 s^{-1} . The same could not be said for the

acrylodan fluorescence, which was only reduced from 1.6 s^{-1} to 1.4 s^{-1} . This is to say that fesselin had a large effect on the disassociation of the actin-myosin complex (as monitored by light scattering) but had very little effect on the rate of the myosin-actin bond breaking. The data from the studies presented in this section definitively show the interaction between fesselin and actin-myosin involves a tethering of the actin and myosin together.

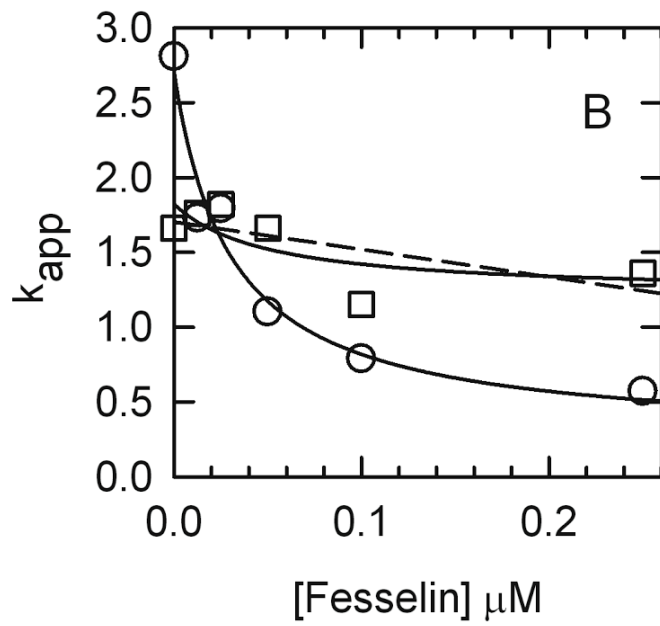
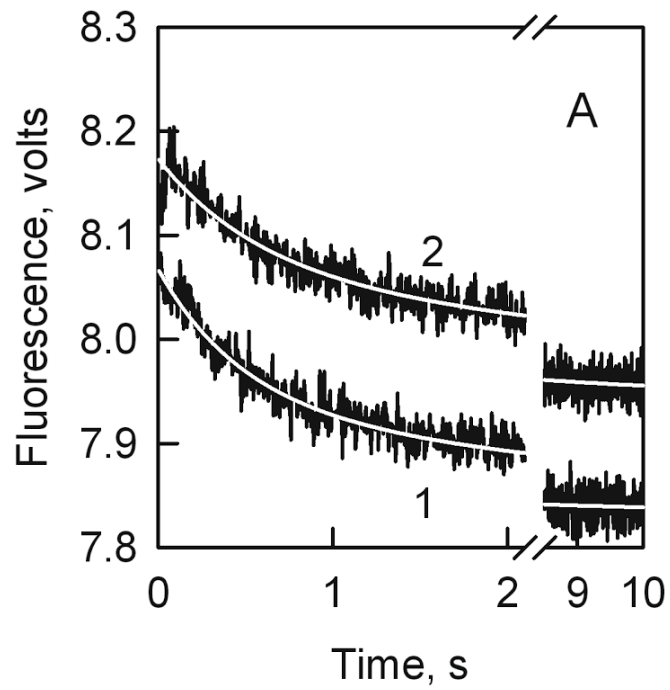


Figure 13

Fesselin had little effect on acrylodan tropomyosin fluorescence following the rapid addition of ATP to the actin–myosin complex. (A) Acrylodan fluorescence transients in the absence of fesselin (for curve 1, $k_1 = 1.6 \text{ s}^{-1}$ and $k_2 = 0.17 \text{ s}^{-1}$) and with $0.25 \text{ }\mu\text{M}$ fesselin (for curve 2, $k_1 = 1.4 \text{ s}^{-1}$ and $k_2 = 0.15 \text{ s}^{-1}$). The fitted curves are shown as white lines on the data traces. (B) Plots of the apparent rate constant for the rapid phase, k_1 , vs. fesselin concentration for light scattering (\circ) and acrylodan fluorescence (\square). Hyperbolic fits are shown for both processes. The best straight line fit to acrylodan fluorescence is also shown as a dashed line. Conditions: 94 mM NaCl, 10 mM MOPS pH 7.0, 2 mM MgCl_2 , 1 mM dithiothreitol, 10°C (Reprinted with permission from Kingsbury et al. copyright 2013 American Chemical Society)

Fesselin stabilizes myosin filaments

The initial work with fesselin focused on its interactions with actin alone. This branched into the studies looking at actin and myosin tethering by fesselin. We also examined the possibility that binding of fesselin to myosin affects the stability of unphosphorylated myosin filaments.

We measured the time course of disassembly of filamentous dephosphorylated smooth muscle myosin by ATP. The binding of ATP to unphosphorylated myosin dissociates filaments into inactive folded myosin monomers (Trybus et al. 1982, Ikebe et al. 1983). Previous studies used negative stain electron microscopy to look at the stabilization of dephosphorylated myosin filaments by caldesmon (Katayama et al. 1995). Katayama et al. found that caldesmon inhibited unphosphorylated smooth myosin filament disassociation. We performed similar experiments to look at the effect of fesselin on smooth myosin filament stability; these experiments initially used stopped-flow rather than electron microscopy. Myosin was rapidly mixed with 4 mM ATP which caused a rapid decrease in voltage.

Figure 14 shows that the light scattering transition from myosin filaments to individual myosin was biexponential, indicating the presence of at least one intermediate in the disassembly process. The two apparent rate constants of disassembly were 1.1 and 0.1 s⁻¹. Increasing concentrations of fesselin decreased both rate constants by similar amounts. At 0.2 μM fesselin, the rate constants were reduced to 0.35 s⁻¹ and 0.03 s⁻¹. The reduction in rate means the myosin filaments are not disassociated as rapidly. This suggests that fesselin stabilized the myosin filaments and is preventing disassociation upon addition of ATP.

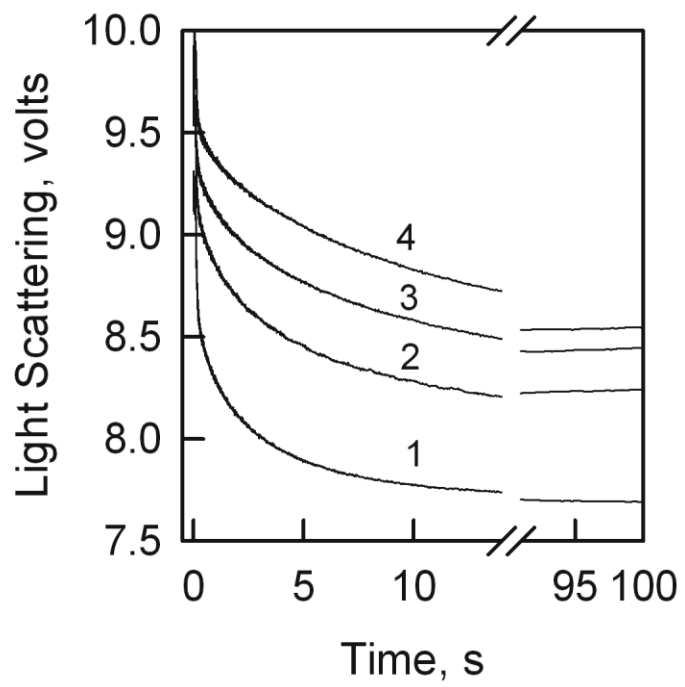


Figure 14

Fesselin reduces the rate of ATP-induced, smooth muscle myosin dissociation. Light scattering transients for 0.05 μM smooth myosin with varying fesselin concentrations were collected. All these transients used 2 mM ATP final. 1) 0 μM fesselin, $k_1 = 1.1 \text{ s}^{-1}$ and $k_2 = 0.10 \text{ s}^{-1}$. 2) 0.05 μM fesselin, $k_1 = 0.51 \text{ s}^{-1}$ and $k_2 = 0.05 \text{ s}^{-1}$. 3) 0.1 μM fesselin, $k_1 = 0.42 \text{ s}^{-1}$ and $k_2 = 0.04 \text{ s}^{-1}$. 4) 0.2 μM fesselin, $k_1 = 0.35 \text{ s}^{-1}$ and $k_2 = 0.03 \text{ s}^{-1}$.

Conditions: 94 mM NaCl, 10 mM MOPS pH 7.0, 2 mM MgCl_2 , 1 mM dithiothreitol, 10°C
(Reprinted with permission from Kingsbury et al. copyright 2013 American Chemical Society)

To confirm the stabilization effects observed by stopped-flow in figure 14, the experiments were repeated using negative stain electron microscopy. This was performed using the same procedure outlined in figure 8, but in the absence of actin. The proteins involved were treated in the same manner as in the light scattering stopped-flow experiments (figures 8 and 14). ATP was added to the protein mixture immediately prior to application on the grid. random fields were selected to evaluate the effect of ATP on the myosin filaments. Myosin filaments were counted and measured as seen in figure 15. In the absence of fesselin, none of the fields showed intact myosin filaments (figure 15 A). When fesselin was present, the myosin filaments were in a normal abundance and similarly sized to normal myosin filaments (myosin filaments without ATP or fesselin),(figure 15 B). This clearly showed similar findings to those described earlier (Katayama et al. 1995) with caldesmon. Fesselin indeed stabilized myosin filaments against ATP-induced disassociation.

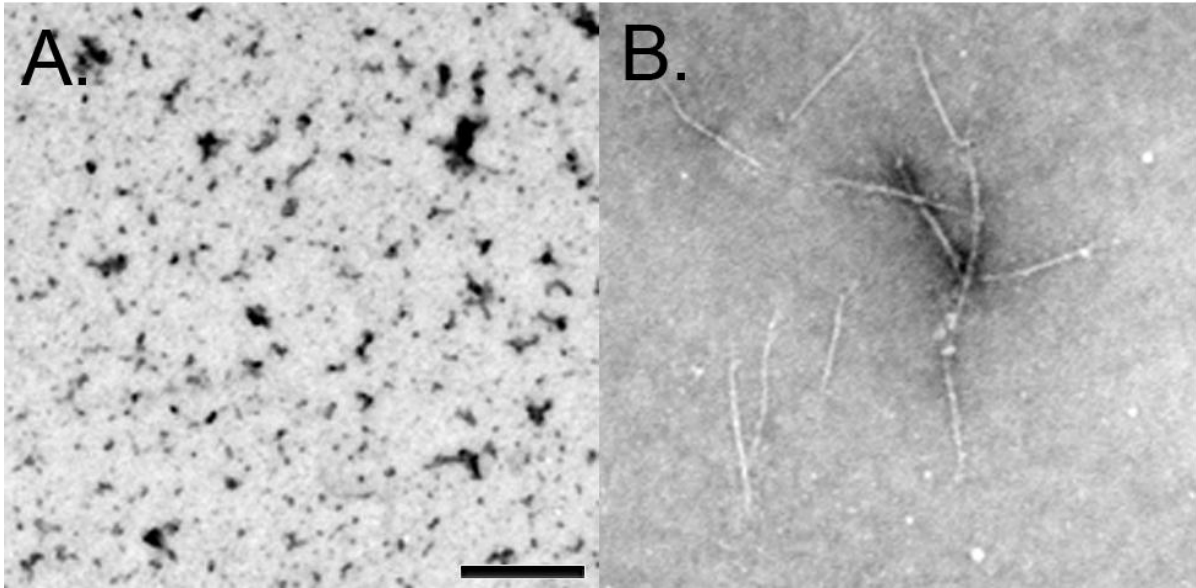


Figure 15

Fesselin stabilized myosin filaments against ATP-induced disassociation shown using electron microscopy. (A) Smooth muscle myosin with ATP. (B) Smooth muscle myosin–fesselin filaments with ATP. Conditions: 0.05 μM smooth muscle myosin, 0.1 μM fesselin, 2 mM ATP, 94 mM NaCl, 10 mM MOPS pH 7.0, 2 mM MgCl_2 , 1 mM dithiothreitol. ATP was added to myosin immediately before it was added to the grid. (Reprinted with permission from Kingsbury et al. copyright 2013 American Chemical Society)

Fesselin increases the length and thickness of myosin filaments

The decrease in light scattering seen in the stopped-flow experiments indicated a reduction in filament size, and it is known from earlier work that this is due to the disassembly of myosin filaments. We examined the effect of fesselin on the structure of myosin filaments to confirm the stabilizing effect of fesselin and to determine the specific structural changes to myosin filaments caused by fesselin.

Figure 16 A shows electron micrographs of unphosphorylated myosin filaments in the absence of fesselin. Filaments were short and with structures similar to previously reported smooth muscle myosin filaments under these conditions (Trybus et al. 1987). The myosin filaments were noticeably larger in the presence of fesselin (figure 16 B). This increase in size did not appear to alter the basic structure of the filaments.

Panels C and D are show the distribution of filament lengths and widths with and without fesselin. The grey lines represent the measurements in the absence of fesselin and the black lines represent the measurements in the presence of fesselin. The lengths of myosin filaments whereas increased greater than two-fold and the widths increased by a similar amount.

In addition to increasing the size of myosin filaments in the presence of fesselin, myosin filaments were bundled together by fesselin as seen in figure 17. The observation of these bundles was found to occur across the fesselin-myosin grids. The myosin filament bundles appear to have end-to-end interactions as well as side-to-side interactions. The observation of myosin bundles added a very interesting aspect to fesselin. The bundling of myosin filaments is novel among smooth muscle proteins.

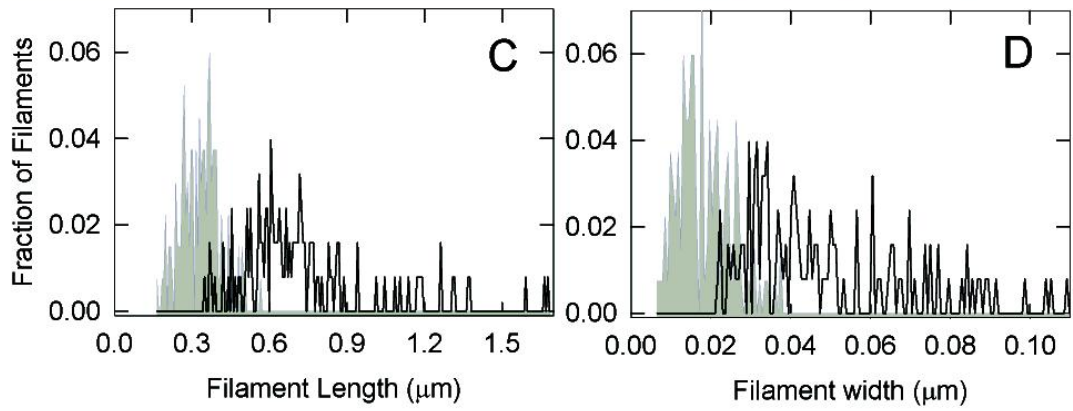
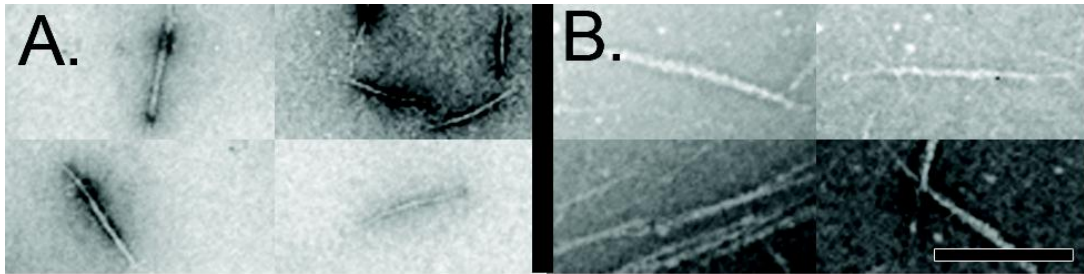


Figure 16

Electron microscopic analysis shows fesselin increases the length and width of smooth muscle myosin filaments. Panels A and B are representative electron micrographs of 0.05 μM smooth muscle myosin in the absence (A) and presence (B) of 0.1 μM fesselin. Distributions of filament lengths (C) and widths (D) were determined by measuring the filaments with NIH ImageJ. These measurements were ordered by size and plotted as size vs. the fraction of filaments at that size. 133 filaments were measured in the absence of fesselin, and 126 filaments were measured in the presence of fesselin. Gray shaded regions are in the absence of fesselin, with an average filament length of 0.32 μm and a width of 0.017 μm . Black lines are in the presence of fesselin, with an average filament length of 0.72 μm and a width of 0.048 μm . (Reprinted with permission from Kingsbury et al. copyright 2013 American Chemical Society)

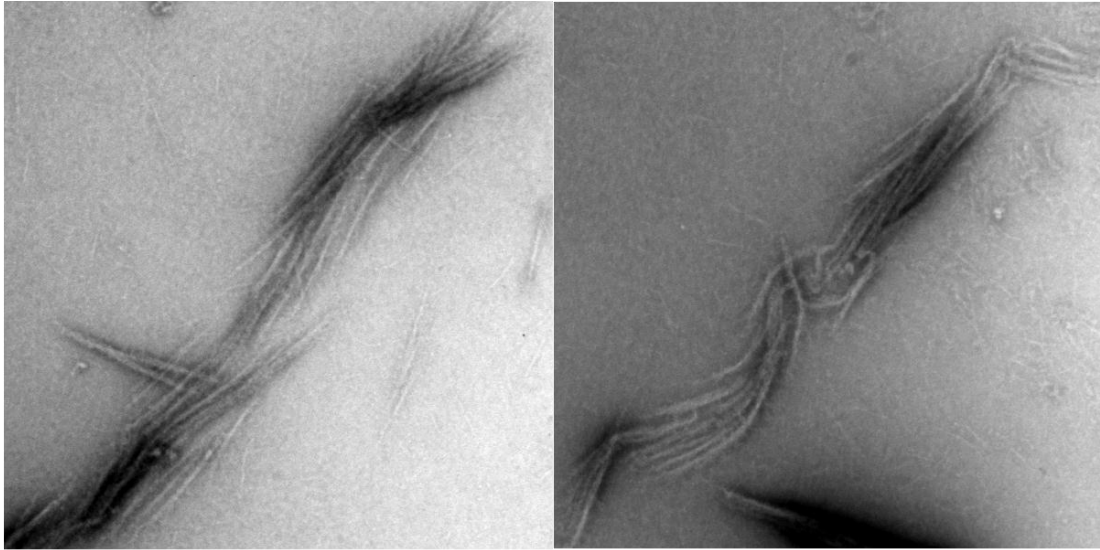


Figure 17

Fesselin bundled myosin filaments into large arrays. Electron microscopy images of 0.05 μM smooth myosin and 0.05 μM fesselin showing the buildup of a large myosin filament arrays. Conditions: 94 mM NaCl, 10 mM MOPS pH 7.0, 2 mM MgCl_2 , 1 mM dithiothreitol, 10°C

Part II. Determination of sites of interaction of fesselin and myosin

Identification of binding sites for the fesselin-myosin interaction.

To further understand how fesselin and myosin interact, the binding sites on myosin were explored using a variety of experimental procedures. The first approach used covalent cross-linking reagents with fesselin and myosin in an attempt to link the binding site on myosin to fesselin. Next sedimentation was used to analyze fesselin peptides responsible for binding to myosin. Finally, myosin affinity chromatography was used to attempt to capture the fesselin peptides that bind to the myosin. These approaches had only limited success and are recorded here for the benefit of future investigations.

Covalent Cross-linking of fesselin and myosin

Covalent cross-linking of fesselin and myosin was attempted using a variety of cross-linking reagents and under a variety of working conditions. The basic procedure involved mixing the bait protein with the cross-linking reagent for a set incubation period and then adding in the prey protein. The first set of experiments used myosin as the bait protein and fesselin as the prey. This was then reversed to use fesselin as the prey.

Difficulties arose in the cross-linking experiments as both fesselin and myosin

have a tendency to self-associate. ATP was added to the mixture to minimize myosin self-association. Even in that condition the cross-linking remained inconclusive. Figure 18 shows the results from select cross-linking reagents. The reagents included: 1-Ethyl-3-(3-dimethylaminopropyl) carbodiimide (EDC), dimethyl 3,3'-dithiopropionimidate dihydrochloride (DMDTPP), and N,N'-1,4-Phenylene-dimaleimide (PPDM). PPDM was the only cross-linking reagent to show potential fesselin-myosin complex cross-linking (lane j). The gel used for figure 18 has a glaring problem as the control (lane a) does not properly show fesselin and myosin together but this gel has the best evidence of cross-linking. (lane h) acting as the myosin control for (lane j) had heavy cross-linking within the stacker hence the absence of a myosin band within the resolving gel. When (lane i) was compared with the other results, there was some evidence of fesselin-fesselin cross-linking when taking into account the expected amount evidenced by (lane c). (lane j) shows the same amount of fesselin decrease and a recovery of some of the myosin band, as well as the appearance of several other protein bands.

The newly apparent bands (lane j) might be a fesselin-myosin cross-linked product. If these studies were continued the determination of fesselin-myosin cross-linked products would be carried out by western blot analysis with fesselin antibodies. After confirmation that fesselin and myosin were present in the complex the experiment would be repeated with a cross-linking reagent containing a retrievable tag. Using the tagged cross-linking reagent the fesselin-myosin complex could be isolated. The isolate could then be digested with proteases and the tag used again to isolate the myosin binding portion of fesselin before analysis by mass-spectrometry.

In my studies an attempt was made to better resolve the myosin cross-linked complexes. The cross-linking experiments were repeated using agarose-acrylamide gel rather than acrylamide alone (figure 18). The agarose-acrylamide gels have a final acrylamide matrix of 3% and the addition of agarose is required to give some stability to the gels. Figure 19 shows the results of various cross-linking reagents reacting with myosin and fesselin. In lanes e – g the experiments with N,N'-1,4-Phenylene-dimaleimide (PPDM) were run on the agarose-acrylamide gel.

The gels collected (figures 18 and 19) showed that there was evidence for several cross-linking products of myosin and fesselin. To discern the origin for each of the products more controls were needed. Figure 20 shows the results of testing the myosin sample alone. This was done to better understand the banding patterns observable in the other experiments. It was clear from looking at lanes a and d that the myosin used for the experiments contained some cross-linked myosin and that the crosslinking in the sample was due to disulfide linkage. Minimizing the time out of reducing agents alleviated this.

The most promising results from the cross-linking studies came from the use of N,N'-1,4-Phenylene-dimaleimide (PPDM). The other reagents used showed no fesselin-myosin cross-linked products whereas the PPDM had evidence of new complexes. These complexes were lighter than the myosin-myosin interactions but heavier than the myosin heavy chain alone.

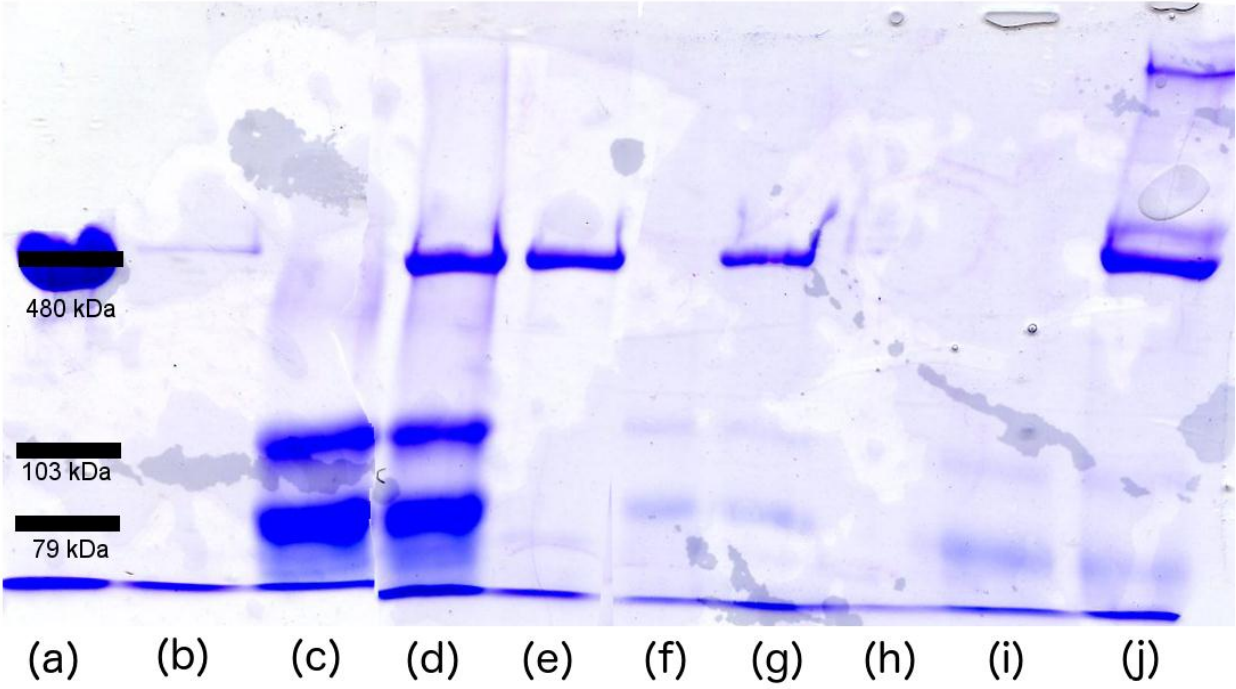


Figure 18

Cross-linking of myosin and fesselin did not yield definitive results. (a) 0.05 μ M Smooth myosin, (b) 0.05 μ M smooth myosin + 1 μ M 1-Ethyl-3-(3-dimethylaminopropyl) carbodiimide (EDC), (c) 0.05 μ M fesselin + 1 μ M EDC (d) 0.05 μ M smooth myosin + 0.05 μ M fesselin + 1 μ M EDC, (e) 0.05 μ M smooth myosin + 1 μ M dimethyl 3,3'-dithiopropionimidate dihydrochloride (DMDTPP), (f) 0.05 μ M fesselin + 1 μ M DMDTPP, (g) 0.05 μ M myosin + 0.05 μ M fesselin + 1 μ M DMDTPP, (h) 0.05 μ M myosin + 1 μ M N,N'-1,4-Phenylene-dimaleimide (PPDM), (i) 0.05 μ M fesselin + 1 μ M PPDM, (j) 0.05 μ M myosin + 0.05 μ M fesselin + 1 μ M PPDM. Conditions: 85 mM NaCl, 10 mM Na_2HPO_4 pH 7.4, 10°C

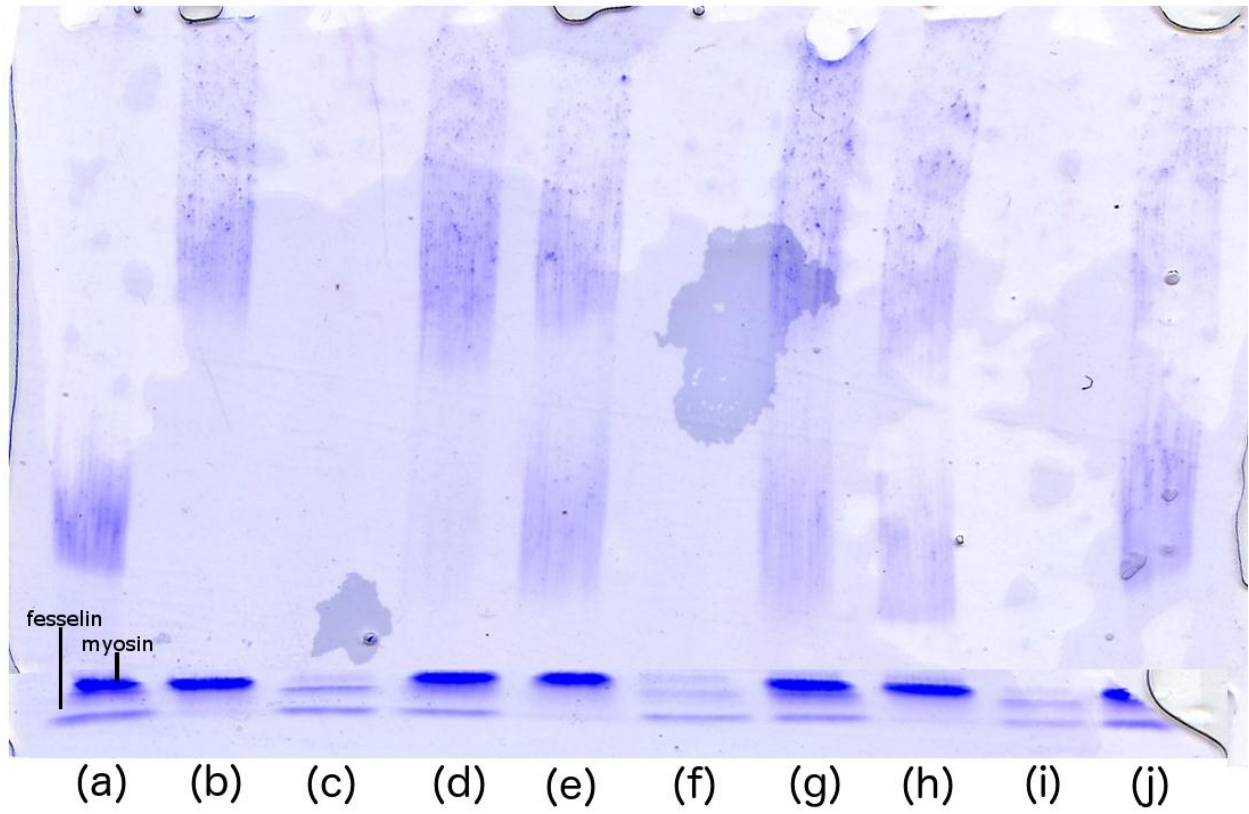


Figure 19

Using agarose-acrylamide gels the large myosin complexes were more readily resolved.

(a) 0.05 μM smooth myosin + 0.05 μM fesselin, (b) 0.05 μM smooth myosin + 1 μM 3,3'-dithiobis(sulfosuccinimidylpropionate) (DTSSP), (c) 0.05 μM fesselin + 1 μM DTSSP, (d) 0.05 μM myosin + 0.05 μM fesselin + 1 μM DTSSP, (e) 0.05 μM myosin + 1 μM N,N'-1,4-Phenylene-dimaleimide (PPDM), (f) 0.05 μM fesselin + 1 μM PPDM, (g) 0.05 μM myosin + 0.05 μM fesselin + PPDM, (h) 0.05 μM myosin + 1 μM Sulfosuccinimidyl-2-(p-azidosalicylamido)ethyl-1,3-dithiopropionate (SASD), (i) 0.05 μM fesselin + 1 μM SASD, (j) 0.05 μM myosin + 0.05 μM fesselin + 1 μM SASD. Conditions: 85 mM NaCl, 10 mM Na_2HPO_4 pH 7.4, 10°C

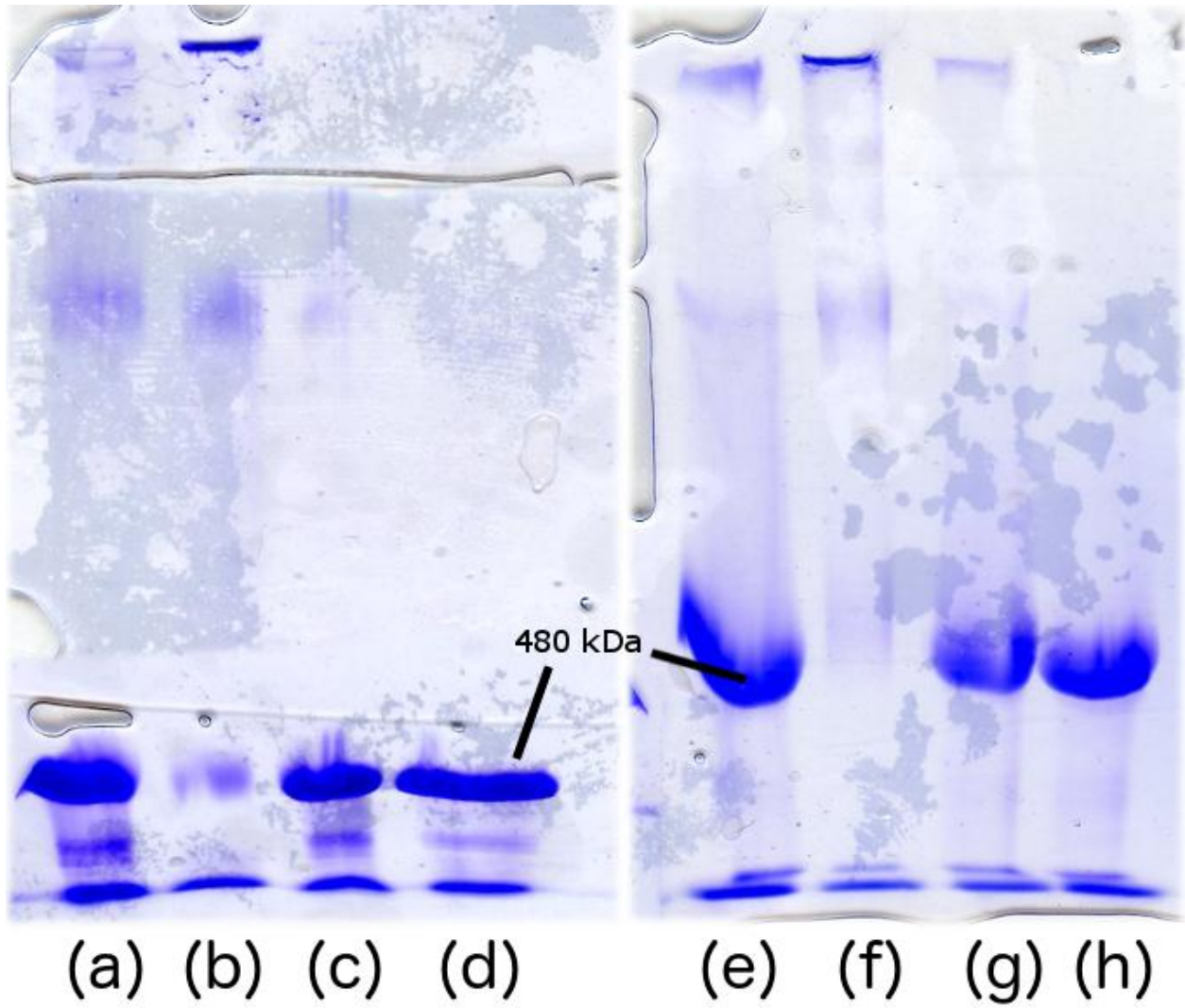


Figure 20

The myosin used in the cross-linking contains cys-cys linked myosin. The myosin was analyzed on both agarose-acrylamide gels as well as normal acrylamide gels. (a) – (d) were analyzed using 3% agarose-acrylamide gel, and (e) – (h) were analyzed using 5% acrylamide gel. (a) 0.05 μ M myosin (36 hours without dithiolthreitol (DTT)), (b) 0.05 μ M myosin + 1 μ M PPDM, (c) 0.05 μ M myosin (12 hours no DTT), (d) 0.05 μ M myosin + 1 mM DTT, (e) 0.05 μ M myosin (36 hours without DTT), (f) 0.05 μ M myosin + 1 μ M PPDM, (g) 0.05 μ M myosin (12 hours no DTT), (h) 0.05 μ M myosin + 1 mM DTT. Conditions: 85 mM NaCl, 10 mM Na₂HPO₄ pH 7.4, 10°C

Fesselin peptide co-sedimentation

To determine what portion of fesselin was binding to myosin, co-sedimentation experiments were attempted. Myosin readily sediments at low speed when placed into a buffer that favors filament formation, under these same conditions fesselin does not sediment. The efficacy of this approach was first tested using intact fesselin. In the absence of myosin, intact fesselin did not appear in the pellet. With myosin and fesselin present the fesselin was found in the pellet. This was determined using SDS-PAGE as myosin and fesselin have a large difference in molecular weight (data not shown).

We repeated this experiment with fragments of full length fesselin. Fesselin was digested with proteases (V8 protease) and the reaction was arrested with protease inhibitors (0.5 mM PMSF) prior to mixing with myosin. The peptide-myosin mixture was then pelleted using centrifugation (6000 g, 7 minutes, 4°C). The supernatants and pellets were analyzed separately by polyacrylamide gel electrophoresis. The gels from the fesselin peptide experiments did not show definitive evidence of a captured fesselin peptide as can be seen in figure 21. The results of this experiment are inconclusive, as it appears the only proteins on the gel are bands correspond to intact fesselin or myosin. To improve on this approach a more extensive V8 protease digestion would be required.

We also tried to measure binding of fesselin fragments to a myosin affinity column. Myosin, HMM or S1 were covalently linked to CNBr activated sepharose 4B. Intact fesselin was successfully bound to affinity columns linked with whole myosin or myosin fragments. The main difference when using intact fesselin for each of the affinity column compositions was the capacity for binding. With the whole myosin a larger

amount of fesselin bound to the column, This was likely because of a lower affinity of fesselin for the myosin fragments. Triton X-100 was included in the buffer when testing all the affinity columns to eliminate issues of non-specific or self-interactions.

The study was repeated using fesselin that was digested with V-8 protease, chymotrypsin, and subtilisin. The peptides were applied directly to the affinity columns. The results of the affinity purification were not definitive (figure 22). After extensive treatment the appearance of extremely faint bands within lanes (h) and (i) can be seen.

The results of this show weak evidence for the capture of myosin binding portions of fesselin. The problem may lie in the method that fesselin uses to bind to targets. Fesselin adapts its shape to suit its target, which may require specific pieces of the protein working in conjunction. Immobilization of the myosin or myosin fragments may have also interfered because of binding to the resin where fesselin needs to bind. Another issue is that the amount recovered and ran on the gel was below the detection level of the staining used. If these experiments were continued a larger sample would be used as well as a more sensitive staining technique such as silver stain.



(a) (b) (c) (d) (e) (f) (g) (h) (i) (j)

Figure 21

Co-sedimentation of intact smooth myosin and fesselin peptides acted to purify remaining intact fesselin in the samples. Samples were prepared by centrifugation at 19,000 rpm for 7 minutes in a TLA 120.1 rotor. The samples were analyzed by SDS-PAGE (15% acrylamide, 19: 1, acrylamide: bis-acrylamide). (a) smooth myosin + digested fesselin, (b) fesselin digest, (c - e) supernatant myosin + digested fesselin, (f) fesselin digest (g - j) pellet myosin + digested fesselin. Conditions: 94 mM NaCl, 10 mM MOPS pH 7.0, 2 mM MgCl₂, 1 mM DTT, 10° C

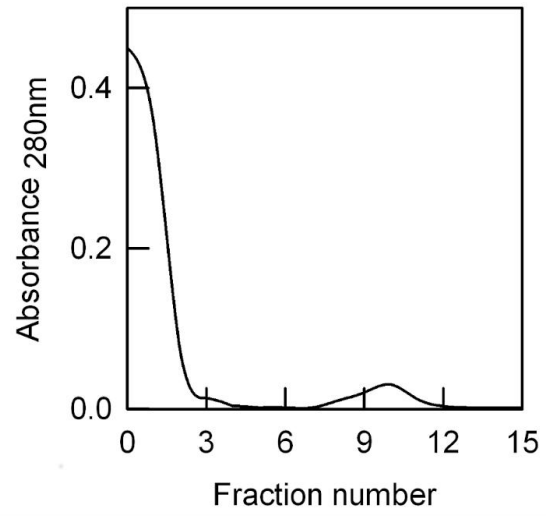
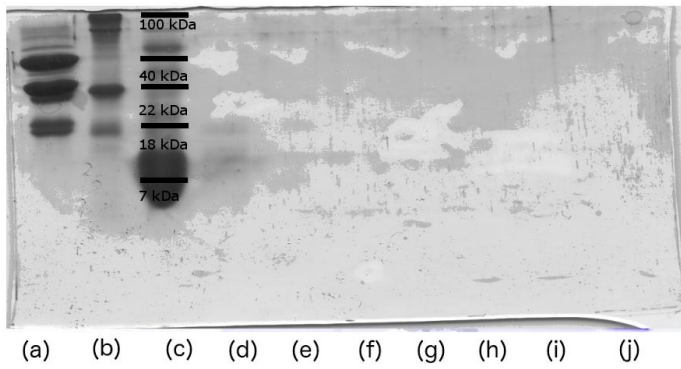


Figure 22

Using myosin and myosin fragments for affinity purification of fesselin fragments proved to be difficult. Myosin or myosin fragments were linked to affinity resin blocked and washed prior to running fesselin digests. The columns were used with 50 mM ionic strength buffer to promote binding. The chart on the right shows the absorbance readings for the affinity column. The fractions were then run on highly cross-linked acrylamide gels (15% acrylamide, 19: 1, acrylamide: bis-acrylamide). (a) human cardiac troponin (37 kDa TnT, 22 kDa TnI, 18 kDa TnC), (b) 100 kDa skeletal myosin subfragment-1, (c) 7 kDa aprotinin, (d) fesselin digest pre-column load, (e – g) wash, (h – j) elution from column

Part III: Regulation of fesselin-myosin binding

The effect of calmodulin on actin and myosin dissociation

If fesselin promotes the assembly of contractile units it is likely that the process is regulated. Indeed, the polymerization of actin by fesselin is strongly inhibited by Ca^{2+} -calmodulin and modestly stimulated by apo-calmodulin (Schroeter et al. 2004, Kolakowski et al. 2004). Because the interaction between fesselin and actin is regulated by calmodulin, we wanted to test the possibility that Ca^{2+} and calmodulin also regulate actin-fesselin-myosin complex dissociation.

To determine the effect of calmodulin on the fesselin-stabilized complex of actin-myosin, we measured the rate of actin-myosin disassociation in the presence of calmodulin and ATP at various concentrations of fesselin using pyrene-actin fluorescence measured by stopped-flow.

In the presence of fesselin and calmodulin the amplitude of pyrene fluorescence for the dissociation of myosin from pyrene-actin was decreased (figure 23 A & B). In contrast fesselin alone did not affect actin-myosin dissociation (figure 23 C & D). With the reduction in the fluorescence amplitude in the presence of calmodulin the next step was to observe the changes as a function of calmodulin concentration.

The next experiments were performed with pyrene-actin with myosin and

fesselin. Various concentrations of calmodulin were then added to this protein mixture (0.2, 2, and 10 μM). The rate of ATP-induced disassociation was determined at each of the calmodulin concentrations using pyrene-actin fluorescence, these experiments were performed at 0.5 mM CaCl_2 and 1 mM EGTA. This was done because calmodulin is a calcium binding protein and its interactions with fesselin are modulated by calcium (figure 24).

The pyrene-actin fluorescence rates (measure of ATP-induced actin-myosin disassociation) were plotted against the calmodulin concentration. In the absence of calcium the rate of dissociation increased from 30.7 s^{-1} to 42.2 s^{-1} as the concentration of calmodulin was increased. In the presence of calcium the rate decreased from 39.5 s^{-1} to 35.6 s^{-1} as the concentration of calmodulin was increased. Figure 23 showed that the presence of calmodulin increased the amplitude of pyrene fluorescence; figure 24 shows that calmodulin also altered the rate of fluorescence change. The change in amplitude shows that in the presence of calmodulin a smaller fraction of the actin-fesselin-myosin proceeded through the reaction (actin-myosin bond breaking). While these effects were not robust, they were consistent and showed changes induced by the presence of calmodulin.

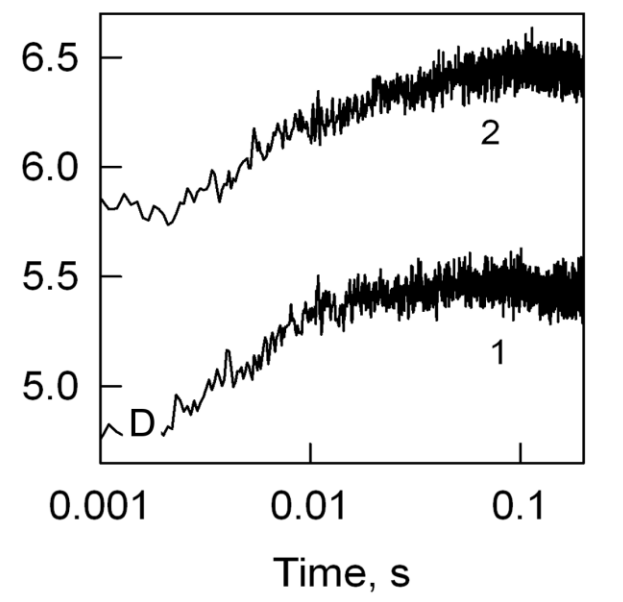
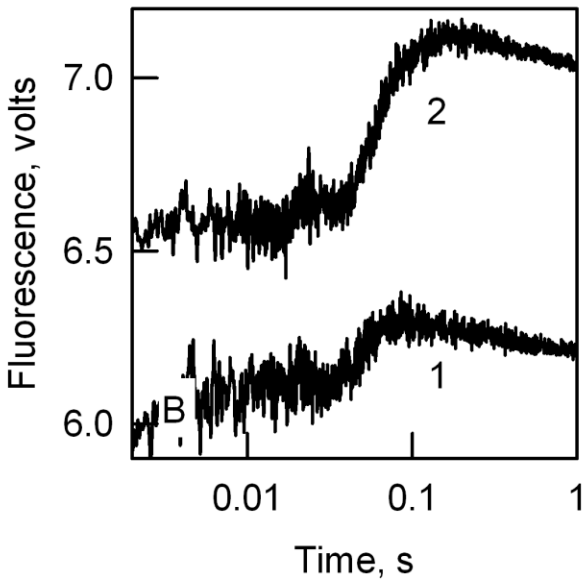
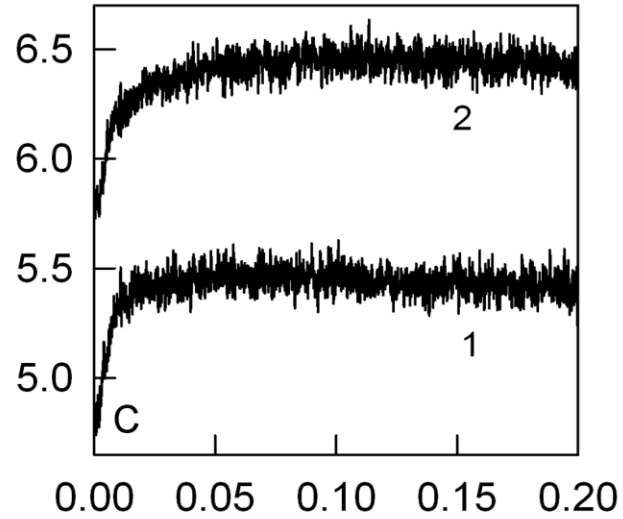
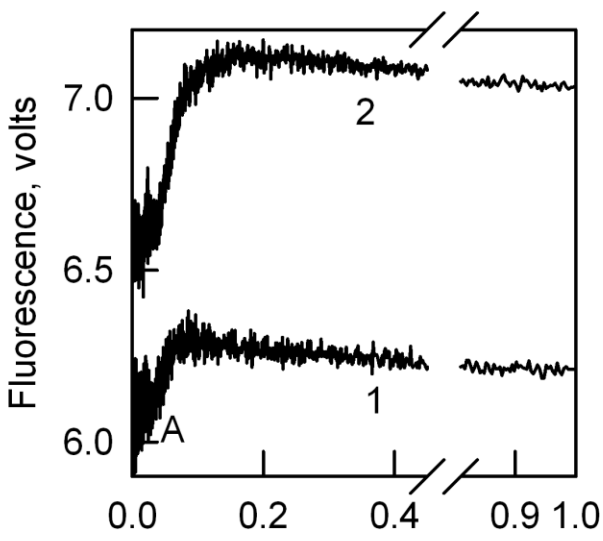


Figure 23

Actin-myosin dissociation induced by ATP in the presence (A, B) and absence (C, D) of calmodulin and presence 0.1 μM fesselin (1) and absence of fesselin (2). Fluorescence stopped-flow transients for 0.4 μM phalloidin-pyrene-actin with 0.1 μM smooth myosin and 0.4 μM calmodulin with and without fesselin mixing with 4 mM ATP. A and C) Linear time scale in the presence and absence of calmodulin, respectively. B and D, Logarithmic time scale in the presence and absence of calmodulin, respectively. Conditions: 94 mM NaCl, 10 mM MOPS pH 7.0, 2 mM MgCl_2 , 1 mM DTT, 10°C.

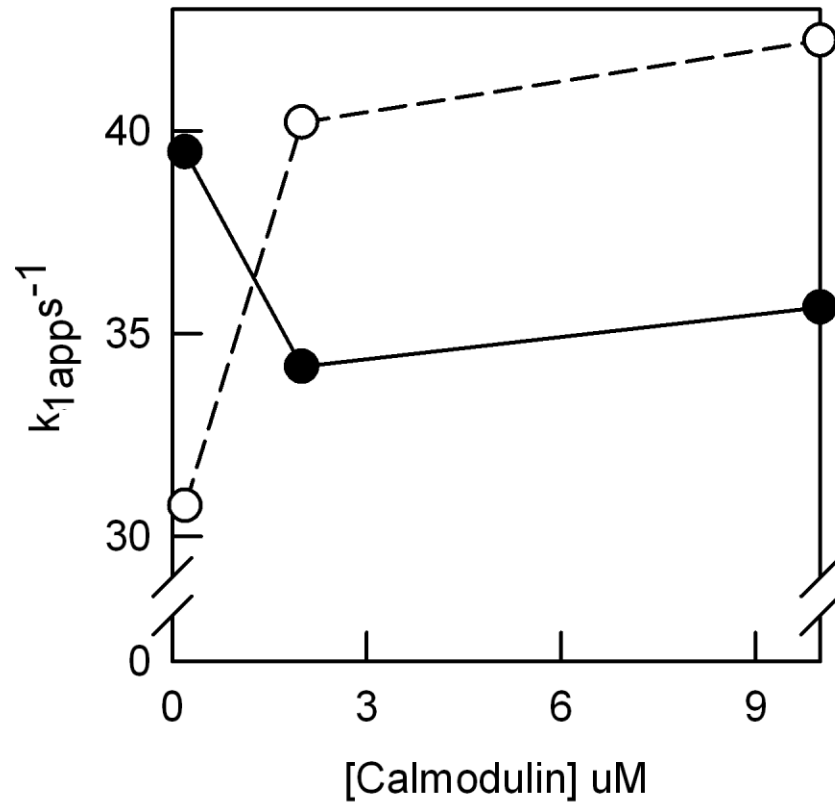


Figure 24

Calmodulin reduces the rate of breaking the actin-myosin bond in the pyrene-labeled actin-fesselin-myosin complex in the presence of 0.5 mM Ca^{2+} (●) but increases the rate in the presence of 1 mM EGTA (○). Pyrene labeled actin, smooth myosin, fesselin, and varying concentrations of calmodulin were rapidly mixed with ATP in the stopped flow device. Pyrene fluorescence was measured and the rate of decrease was plotted against calmodulin concentration. (0.2 μM -10 μM). The rate of dissociation decreases in the presence of calcium and increases in the absence.

IANBD fesselin binding to myosin fragments

The fluorescence experiments presented earlier employed probes that could monitor actin changes (pyrene-actin, acrylodan-tropomyosin), or probes that could monitor myosin changes (fluorescein-myosin). Fluorescently labelled fesselin was generated in order to directly determine fesselin binding.

Fesselin contains seven cysteine residues positioned throughout the protein; because fesselin is natively unfolded these cysteine residues are all readily available under the experimental conditions. The probe used for the labeling procedure was N,N'-dimethyl-N-(iodoacetyl)-N'-(7-nitrobenz-2-oxa-1,3-diazol-4-yl)ethylenediamine (IANBD).

The binding of S-1 and IANBD-fesselin in the presence of calmodulin (figure 25 B) was found to be faster without Ca^{2+} (curve 2) with apparent rate constants of $k_1 = 17.34 \text{ s}^{-1}$ and $k_2 = 1.55 \text{ s}^{-1}$. In the presence of 0.5 mM Ca^{2+} (curve 1) the rates decreased to 8.90 s^{-1} and 0.374 s^{-1} . The decrease could be due to folding of fesselin induced by Ca^{2+} -calmodulin competing with the S-1 for binding.

The experiments were also performed with intact smooth myosin. The binding of myosin and IANBD-fesselin in the presence of calmodulin (figure 25 A) was found to be biphasic without calcium (curve 1) with a $k_1 = 20.75 \text{ s}^{-1}$ and $k_2 = 2.64 \text{ s}^{-1}$. With 0.5 mM Ca^{2+} present (curve 2) the first apparent rate constant remained much the same $k_1 = 19.04 \text{ s}^{-1}$ while the second increased by greater than 4-fold to $k_2 = 11.23 \text{ s}^{-1}$. The presence of Ca^{2+} -calmodulin (curve 2) caused the voltage to peak then decrease at around 0.15 seconds, this pattern was absent with apo-calmodulin.

The effects of calmodulin observed by IANBD-fesselin fluorescence appear to be inhibition of myosin bundling. When this experiment is monitored by light scattering the

bundling of myosin by fesselin is regulated by calcium (figure 26). The fluorescence changes induced by Ca^{2+} -calmodulin could be explained as a folding change (this folding was seen as a fluorescence change represented as F^* going to F^{**}) in the fesselin due to calmodulin binding (figure 27).

The binding of fesselin to myosin or S-1 was measured across multiple myosin concentrations by stopped-flow in the presence of calcium. The resulting rates were then plotted against total concentration of myosin or S-1 in the experiment (figure 28). The rates plotted were the first rate process as the concentration of myosin or S-1 had the most effect on it. From the plots of the rate versus the concentration, the affinity of the IANBD-fesselin for myosin was estimated. The affinity for myosin was reduced from $0.5 \mu\text{M}$ as described earlier (Schroeter et al. 2008) to nearly $2 \mu\text{M}$. This finding shows that the labeling of fesselin with fluorescent probes impacted its ability to bind myosin.

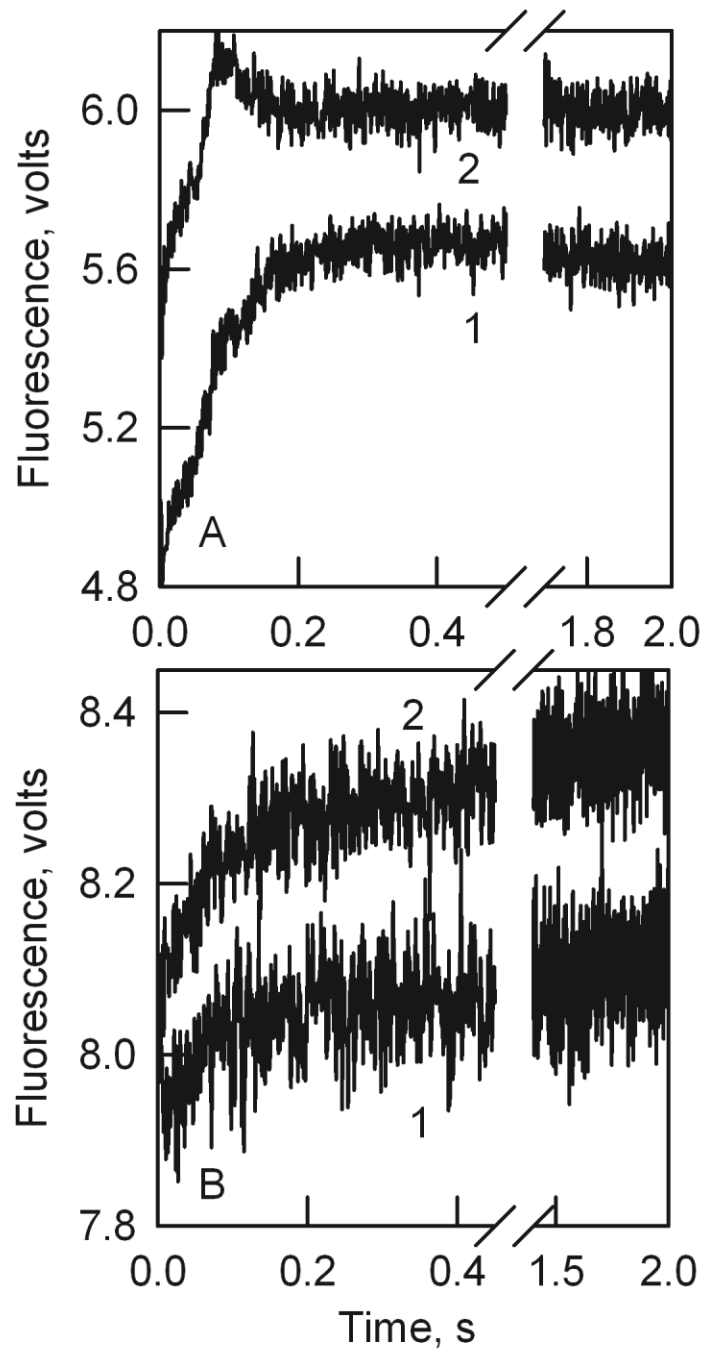


Figure 25

Binding of IANBD-labeled fesselin to myosin in the presence of calmodulin. IANBD labeled fesselin and calmodulin were rapidly mixed with either myosin and calmodulin (A) or myosin subfragment-1 (S-1) and calmodulin (B) in the presence of 1 mM EGTA (1) or 0.5 mM CaCl_2 (2) **A)** Final concentrations, 0.05 μM fesselin, 0.5 μM myosin, 0.05 μM calmodulin, 1) 1 mM EGTA, $k_1 = 20.75 \text{ s}^{-1}$ and $k_2 = 2.64 \text{ s}^{-1}$, 2) 0.5 mM CaCl_2 , $k_1 = 19.04 \text{ s}^{-1}$ and $k_2 = 11.23 \text{ s}^{-1}$. **B)** Final conditions, 0.05 μM fesselin, 0.5 μM S-1, 0.05 mM calmodulin, 1) 0.5 mM CaCl_2 , $k_1 = 8.90 \text{ s}^{-1}$ and $k_2 = 0.374 \text{ s}^{-1}$, 2) 1 mM EGTA, $k_1 = 17.34 \text{ s}^{-1}$ and $k_2 = 1.55 \text{ s}^{-1}$. Conditions: 94 mM NaCl, 10 mM MOPS pH 7.0, 2 mM MgCl_2 , 1 mM dithiothreitol, 10°C.

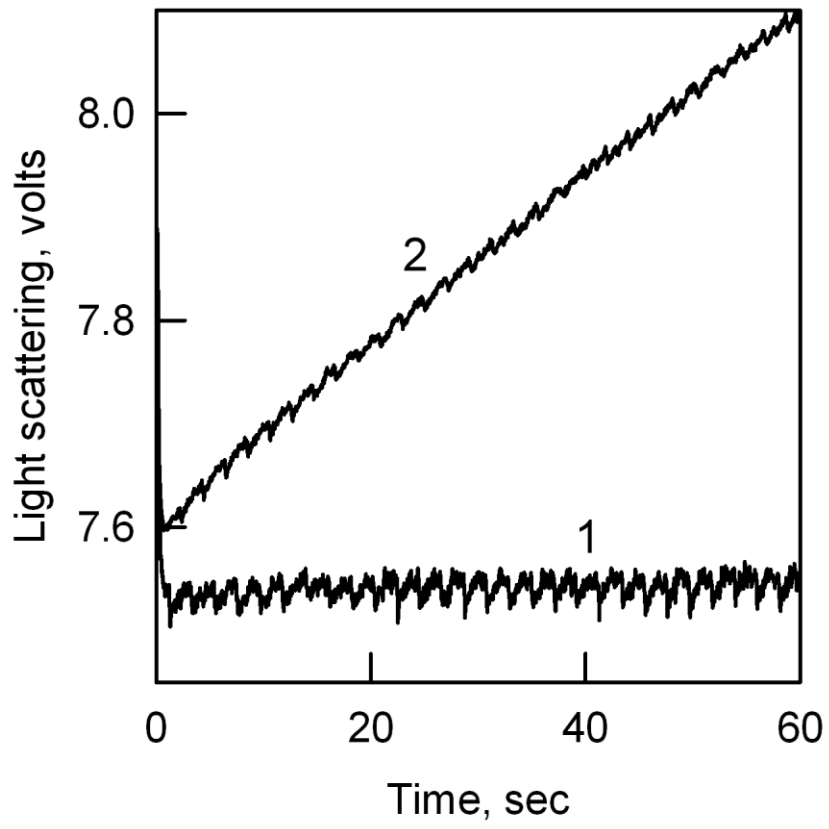


Figure 26

Light scattering measurements of myosin bundling by IANBD-fesselin in the presence of calmodulin. For these experiments the final protein concentrations were: 0.05 μM fesselin, 0.5 μM myosin and 0.05 μM calmodulin. Curve 1 is in the absence of Ca^{2+} (1 mM EGTA). Curve 2 is the bundling in the presence of 0.5 mM CaCl_2 the increase in signal is likely due to myosin bundle formation. The bundling of fesselin appears to be inhibited in the absence of Ca^{2+} .

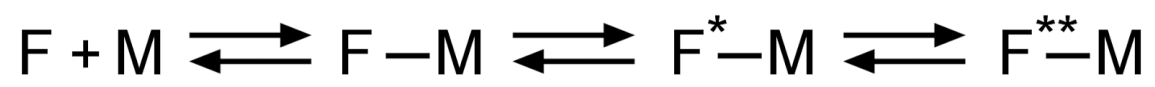


Figure 27

Scheme used for the modeling of IANBD-fesselin fluorescence changes induced by Ca^{2+} -calmodulin. The binding of fesselin and myosin causes a fluorescence change. The differences with and without Ca^{2+} can be explained with two fluorescence steps (F^* and F^{**}) where the rate between these two is altered by the Ca^{2+} induced folding.

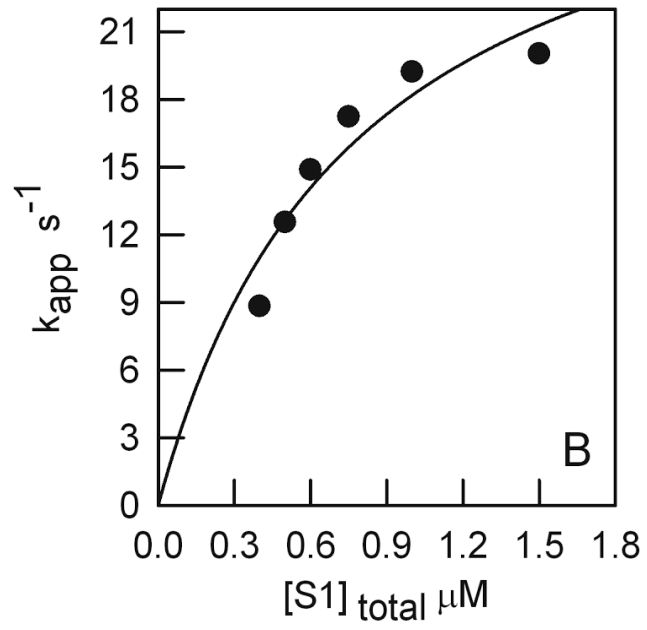
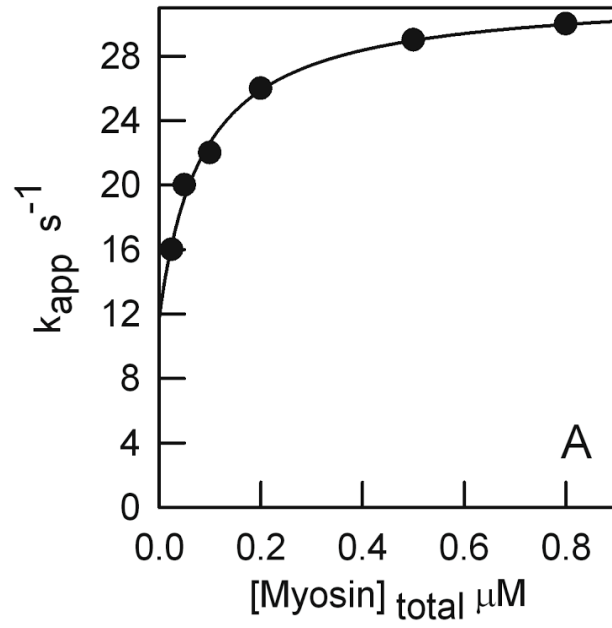


Figure 28

Using IANBD-fesselin the binding kinetics to both smooth myosin subfragment-1 (S-1) and intact smooth myosin were observed. A) IANBD-fesselin + S-1 across various concentrations of S-1. B) IANBD-fesselin + myosin across various concentrations of myosin. The binding of fesselin appears to have been weakened ($<2 \mu\text{M}$) compared to previously measured values ($0.5 \mu\text{M}$). Conditions: 94 mM NaCl, 10 mM MOPS pH 7.0, 2 mM MgCl_2 , 1 mM dithiothreitol, 10°

Discussion

A basic requirement for muscle contraction is the organization of actin and myosin filaments. For productive contraction to occur actin filaments need to be bundled and organized to transmit the force produced by myosin. Our lab and others have already found that fesselin polymerizes F-actin filaments (Beall et al. 2001, Leinweber et al. 1999), and organizes the filaments into bundles (Schroeter et al. 2013). It was also found that the polymerization of actin by fesselin was regulated by Ca^{2+} -calmodulin (Schroeter et al. 2004, Kolakowski et al. 2004).

We have shown here that in addition to the interactions with actin, fesselin also plays an important role in myosin organization. For proper force production myosin must be in filamentous form and in contact with actin filaments. We found that fesselin stabilized unphosphorylated smooth myosin against ATP-induced disassociation. In addition to stabilizing myosin, fesselin was also found to enhance myosin filament length and width as well as organize the filaments into bundles. We have also shown here that fesselin organized actin and myosin filaments by tethering the actin and myosin filaments together.

In addition to the organization of actin and myosin filaments the studies presented here found that the interactions between fesselin and myosin are regulated similarly to the actin-fesselin interactions. It was found that the binding of fesselin to myosin was regulated through Ca^{2+} -calmodulin. The regulation of both the fesselin-

actin and fesselin-myosin activities by calmodulin places fesselin into the role of organizing smooth muscle proteins for contraction.

Fesselin stabilizes myosin

The studies presented here showed that fesselin stabilizes unphosphorylated smooth myosin filaments. Stabilization of smooth myosin filaments is an important interaction because in the case of unphosphorylated smooth myosin, the filaments disassociate when they come in contact with ATP (Suzuki et al. 1978, Trybus et al. 1982, Ikebe et al. 1983). We showed that when fesselin is present the smooth myosin filaments were more resilient to this disassociation.

The stability of unphosphorylated myosin filaments was initially tested using stopped-flow kinetic measurements. As the concentration of fesselin was increased the rate of myosin filament break up slowed. Light scattering traces were collected by stopped-flow and the rate of ATP-induced disassociation was determined. It was observed that the rate of ATP-induced disassociation was not only slower in the presence of fesselin but also ended at higher amplitude. The rate decrease is due to fesselin slowing of the myosin break down. The higher amplitude could be due to multiple populations of myosin that break apart at different rates. The stopped-flow measurements were then confirmed using electron microscopy. The confirmation came when in the presence of fesselin, myosin filaments were present on the ATP treated grids. In the absence of fesselin, myosin filaments were not seen in the presence of ATP.

In addition to stabilizing myosin filaments, fesselin was also found to enhance and organize the smooth myosin filaments. The enhancement of myosin filament length and width was observed by electron microscopy in the absence of ATP. Further examination of the electron microscopy grids found that, in the presence of fesselin, the smooth myosin filaments also formed large bundles. These myosin filament bundles are clearly constructed of individual smooth myosin filaments interacting in an end-to-end and side-to-side manner. The increased size and bundling of myosin filaments when taken with the stabilization of myosin gives more insight into the changes in amplitude noted in the stopped-flow experiments. The increased amplitude is likely from the larger myosin filaments at the starting point, showing indeed there are several populations of myosin filaments.

The findings that fesselin stabilizes unphosphorylated myosin and enhances the filament dimensions have been seen in other proteins, such as telokin (Kudryashov et al. 2002) and caldesmon (Katayama et al. 1995) in smooth muscle. Both caldesmon and telokin interact with the myosin to promote filament formation. This was not seen with fesselin. The filaments formed in the presence of caldesmon and telokin are larger than the average myosin filament (Katayama et al. 1995), but the interactions of these proteins has not been shown to bundle myosin filaments as fesselin has been shown here to do. Additionally the increase in smooth myosin filament size by caldesmon was to a lesser extent than fesselin. With this information it is clear that fesselin is a potent myosin organizing protein in smooth muscle.

Fesselin organizes actin-myosin

With the previous studies showing that fesselin organized both actin and myosin filaments separately we set about testing the ability of fesselin to organize actin and myosin filaments together. As noted previously, for muscle contraction to be possible actin and myosin filaments need to be associated into an organized complex. The results presented here show that fesselin organizes F-actin and myosin filaments together and holds them in close proximity to each other.

The initial evidence for fesselin cross-linking of actin and myosin by fesselin was noted in the light scattering experiments; the ATP-induced disassociation of the actin-myosin complex was slowed in the presence of fesselin. The slowing of the complex break down is clearly due to fesselin interacting with actin and myosin. The actin-myosin complex cross-linking by fesselin was further examined using electron microscopy. The electron microscopy experiments showed that in the presence of fesselin, myosin filaments remain in proximity to the F-actin filaments even in the presence of ATP.

The next finding was that the cross-linking of F-actin and myosin by fesselin was a tethering effect. The binding to both proteins by fesselin did not inhibit normal breaking of the myosin-actin bond by ATP. The tethering of F-actin and myosin by fesselin is schematically laid out in figure 29. Actin (A) and myosin (M) are associated with each other, fesselin (F) binds to both the actin and myosin. ATP binding to myosin causes the actin-myosin bond to break. The tethering come into play as the actin and myosin are being held together through the fesselin. The fesselin-myosin bond then breaks allowing the complex to fully disassociate.

The first evidence for tethering actin and myosin by fesselin was observed in the stopped-flow experiments examining heavy meromyosin (HMM) detachment from actin

by ATP. These experiments showed that fesselin did not significantly slow the detachment rate of HMM. The effects of fesselin on HMM are important as it shows the binding of fesselin is likely strongest in the filament forming portion of myosin (the portion HMM lacks), this experiment further showed that fesselin did not impact the rate of the actin-myosin bond breaking. The next experiments were performed using pyrene labeled actin to more directly monitor the rate of the myosin-actin bond breaking. The pyrene-actin experiments showed very little change in the fluorescence rate with or without fesselin. From this finding it can be concluded to mean that fesselin does not slow the breaking of the actin-myosin bond.

The definitive proof for the tethering interaction of fesselin came when acrylodan tropomyosin was added to the actin-myosin complex. This study used acrylodan fluorescence to monitor the myosin-actin bond in addition to light scattering measurements. The acrylodan-tropomyosin studies showed that the light scattering rates were decreased as shown earlier, but the fluorescence was fairly constant across fesselin concentration. The decrease in the rate of light scattering showed that the particle (tropomyosin-actin-fesselin-myosin) was disassociating more slowly, while the fluorescence (acrylodan-tropomyosin) showed that the rate of the actin-myosin bond breaking was the same with and without fesselin present.

Similar cross-linking of F-actin to myosin has been found with other proteins across muscle types. These include myosin-binding protein-C in striated muscle (Luther et al. 2011) as well as caldesmon (Ikebe et al. 1988, Marston et al. 1992, Chalovich et al. 1988) and calponin (Roman et al. 2013) in smooth muscle. Comparatively the tethering of F-actin and myosin by fesselin is far more robust than that of caldesmon or

calponin. Dr. Chalovich and Dr. Schroeter performed stopped-flow experiments to directly compare the effects of caldesmon and fesselin. The results of this study can be seen in figure 30.

The direct linking of actin and myosin fills a vital role within muscle. In the case of smooth muscle and non-muscle, tethering of the myosin and actin together can fill many of the gaps that exist because there is not a highly defined sarcomere structure as there is in striated muscle. In striated muscle the tethering activity of myosin-binding protein-C is thought to tie the movement of the thick and thin filaments together coordinating the contraction more efficiently (Luther et al. 2011). The results presented here show that fesselin fills an important role within smooth muscle to robustly tether actin and myosin together.

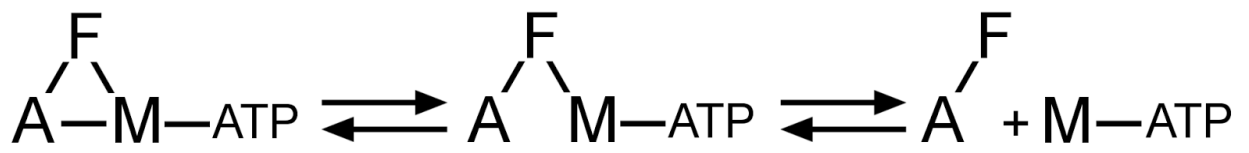


Figure 29

Schematic representation of the actin-fesselin-myosin interaction. Fesselin tethers actin and myosin together. Upon the binding of ATP to myosin, the myosin-actin bond breaks. The fesselin acts as a tether holding the actin and myosin in proximity until the fesselin myosin bond breaks.

The activities of fesselin are regulated by calmodulin

In addition to the findings that fesselin stabilized myosin filaments and organized actin and myosin filaments together it was further found that the binding of fesselin to myosin was regulated by calmodulin. In addition to altering the binding of fesselin and myosin, the myosin bundling activity of fesselin was inhibited in the presence of apo-calmodulin. These findings place fesselin within the Ca^{2+} -signaling pathway presented in earlier. Fesselin would fit in after calmodulin binds calcium and would branch off to alter fesselin interactions with actin and myosin in preparation for contraction (figure 30). Previously published data observed that Ca^{2+} -calmodulin inhibited the ability for fesselin to polymerize F-actin (Schroeter 2004). The findings here show the opposite effect on fesselin-myosin interactions. The calmodulin regulation of fesselin may act as a switch to promote myosin bundling when calcium is high and promote actin polymerization when calcium is low.

The first evidence for calmodulin regulation of fesselin-myosin interactions was found when calmodulin was added to pyrene-actin-myosin stopped-flow experiments. When calmodulin was present with fesselin the pyrene-actin fluorescence decreased in amplitude, meaning that Ca^{2+} -calmodulin caused a smaller portion of the reaction to progress normally. This result was then compared with the observations made of pyrene-actin fluorescence without calmodulin. The results of these experiments showed that in the presence of calmodulin and fesselin the rate of the myosin-actin bond breaking was slowed. After this observation the concentration dependence of calmodulin was tested. The rates of pyrene fluorescence were plotted against

calmodulin concentration. From this set of experiments it would appear that in the presence of Ca^{2+} -calmodulin, fesselin inhibits the disassociation of actin-myosin marginally better than with apo-calmodulin.

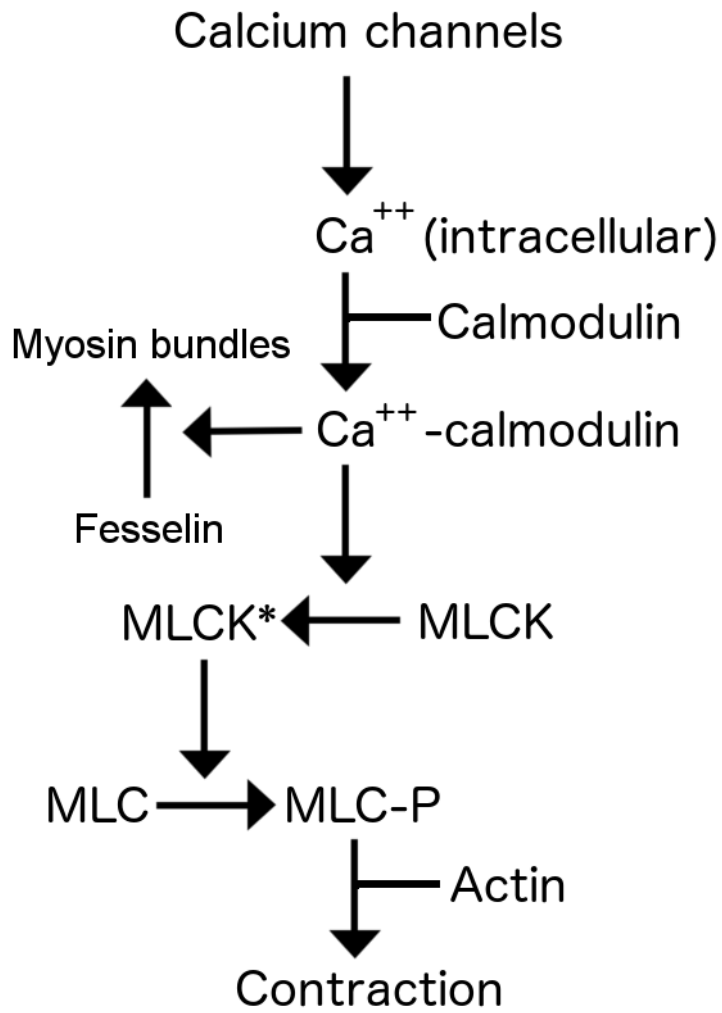


Figure 30.

A simplified schematic of smooth muscle regulation with the additional fesselin-myosin regulation. Calcium channels on the cell allow intracellular calcium ion increase leading eventually to contraction through interaction of Ca^{2+} -calmodulin and MLCK. In addition to MLCK, Ca^{2+} calmodulin appears to interact directly with fesselin and promote the formation of myosin bundles.

Additional evidence for the calmodulin regulation of fesselin came when looking at the binding of IANBD labeled fesselin to myosin. It was found that Ca^{2+} -calmodulin caused a change in the folding of fesselin upon binding to myosin. These binding events can be seen in the fluorescence changes of the IANBD probe the initial rise in fluorescence shows that the probes on the fesselin are being protected.

The evidence for the effect of Ca^{2+} -calmodulin on the bundling of myosin by fesselin was observed when fluorescent fesselin was added to myosin in the presence of calmodulin. When Ca^{2+} was present the signal increased steadily indicating the formation of myosin bundles. When Ca^{2+} was absent the signal remained low. These measurements were taken in conjunction with the fluorescence measurements showing fesselin was still binding the myosin in the absence of Ca^{2+} , but not bundling myosin filaments.

There are a large variety of proteins that are regulated through calcium or calmodulin. The regulation of smooth myosin is an example of this interaction, where calmodulin stimulates phosphorylation and activation of the myosin. The experiments presented here have shown that the interactions between fesselin and myosin are similarly promoted by Ca^{2+} -calmodulin.

Conclusions

The work presented in this discussion reveals that fesselin plays an important role in the organization of actin and myosin filaments, that fesselin stabilizes myosin filaments and has its activity regulated by calmodulin. These activities are summarized

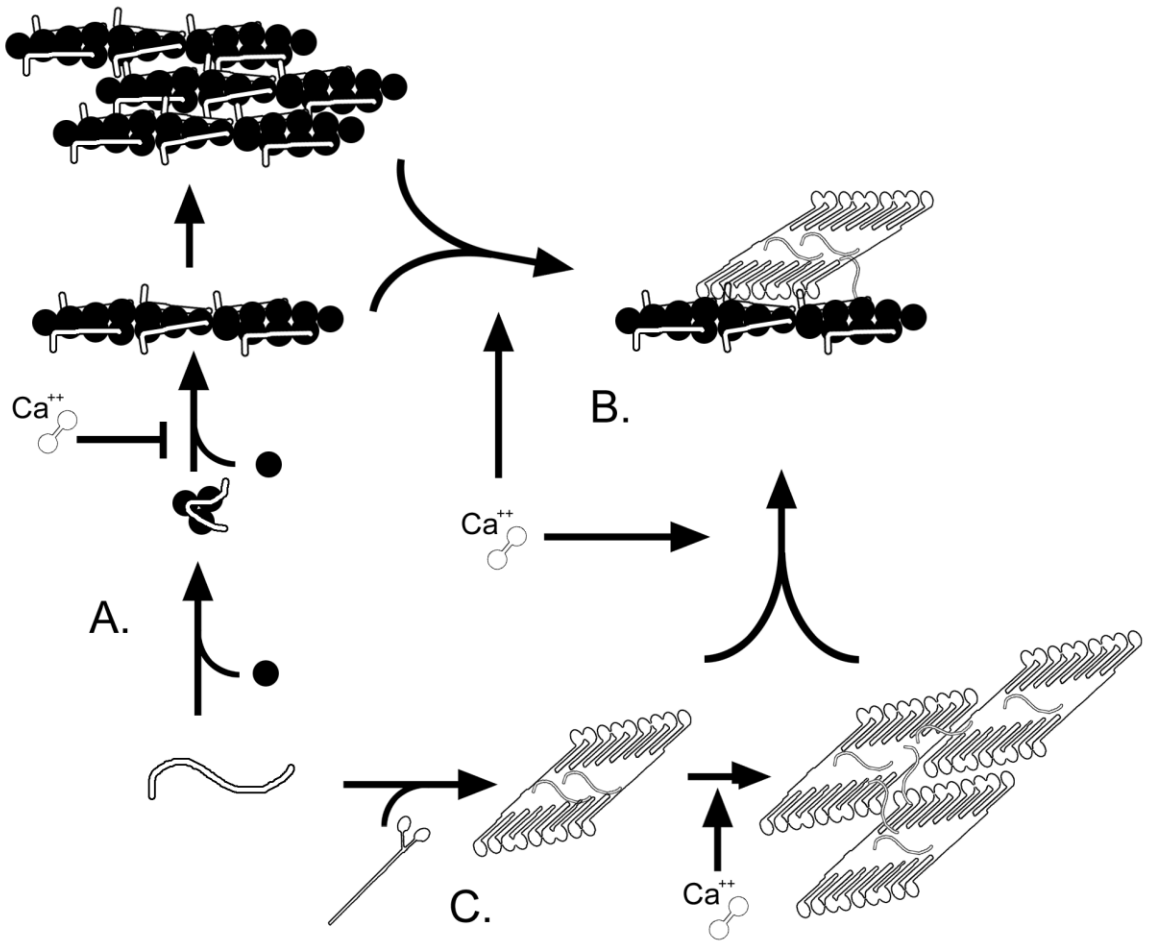
in figure 31 and fit fesselin within the overall regulation of smooth muscle making it a critical protein within the cell.

Future Directions

The studies presented here have shown the interactions of fesselin with smooth muscle myosin. To build upon this, it is important to look at the interactions between fesselin and non-muscle myosin isoforms. This direction is important to definitively understand the role that fesselin plays in cancer cell metastasis.

Another research direction is to define the points of contact between fesselin and myosin. This was attempted in the studies presented here but was unsuccessful despite numerous attempts. To accomplish this task an expressible form of fesselin needs to be generated to more easily control the fragments used for the experiments.

Further studies can also be done involving the regulation of fesselin's activity by calmodulin. These experiments would look at the interaction of fesselin to the other known binding partners in the presence and absence of calmodulin. It is likely that many of fesselin's interactions are regulated by calmodulin.



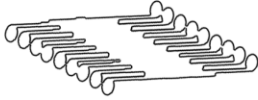
 Fesselin	 Smooth myosin filament
 Calcium calmodulin	 actin monomer
 Smooth myosin	 actin filament

Figure 31.

Proposed activities of fesselin with actin and myosin. A) Fesselin's known interactions with actin. Fesselin binds to actin and accelerates the polymerization, the acceleration is regulated by Ca^{2+} -calmodulin. The fesselin further interacts with actin filaments and bundles them. B) The proposed interaction between fesselin and actin-myosin with the added regulation by Ca^{2+} -calmodulin. C) The proposed interactions of fesselin with myosin. This proposed activity is based on interactions of similar proteins and the affinity of fesselin for myosin.

References

- 1) Ackermann M., K. A. (2011). Myosin binding protein-C: A regulator of actomyosin interaction in striated muscle. *Journal of Biomedicine and Biotechnology*, 2011(Article ID 636403)
- 2) Andorf, C. M., Honavar, V., & Sen, T. Z. (2013). Predicting the binding patterns of hub proteins: A study using yeast protein interaction networks. *PLoS One*, 8(2), e56833. doi:10.1371/journal.pone.0056833; 10.1371/journal.pone.0056833
- 3) Bajpai, V. K., Mistriotis, P., Loh, Y. H., Daley, G. Q., & Andreadis, S. T. (2012). Functional vascular smooth muscle cells derived from human induced pluripotent stem cells via mesenchymal stem cell intermediates. *Cardiovascular Research*, 96(3), 391-400. doi:10.1093/cvr/cvs253; 10.1093/cvr/cvs253
- 4) Beall, B., & Chalovich, J. M. (2001). Fesselin, a synaptopodin-like protein, stimulates actin nucleation and polymerization. *Biochemistry*, 40(47), 14252-14259.
- 5) Borrego-Diaz E., C. J. (2012). Kinetics of regulated actin transitions measured by probes on tropomyosin. *Biophys J.*, 102(5) doi:10.1016/j.bpj.2010.02.030
- 6) Burgess, S. A., Yu, S., Walker, M. L., Hawkins, R. J., Chalovich, J. M., & Knight, P. J. (2007). Structures of smooth muscle myosin and heavy meromyosin in the folded, shutdown state. *Journal of Molecular Biology*, 372(5), 1165-1178. doi:10.1016/j.jmb.2007.07.014
- 7) Craig, R., & Megerman, J. (1977). Assembly of smooth muscle myosin into side-polar filaments. *The Journal of Cell Biology*, 75(3), 990-996.

- 8) Cross, R. A., Geeves, M. A., & Kendrick-Jones, J. (1991). A nucleation--elongation mechanism for the self-assembly of side polar sheets of smooth muscle myosin. *The EMBO Journal*, 10(4), 747-756.
- 9) de la Cuesta, F., Zubiri, I., Maroto, A. S., Posada, M., Padial, L. R., Vivanco, F., Barderas, M. G. (2013). Deregulation of smooth muscle cell cytoskeleton within the human atherosclerotic coronary media layer. *Journal of Proteomics*, 82C, 155-165. doi:10.1016/j.jprot.2013.01.032; 10.1016/j.jprot.2013.01.032
- 10) Diane Proudfoot, C. S. (2012). Human vascular smooth muscle cell culture.. *Methods in Molecular Biology*, 806, 252-263.
- 11) Hemric, M.E., Chalovich, J. M. (1988) Effect of caldesmon on the ATPase activity and the binding of smooth and skeletal myosin subfragments to actin. *JBC* 263 pp1878-1885
- 12) Herrera, A. M., McParland, B. E., Bienkowska, A., Tait, R., Pare, P. D., & Seow, C. Y. (2005). 'Sarcomeres' of smooth muscle: Functional characteristics and ultrastructural evidence. *Journal of Cell Science*, 118(Pt 11), 2381-2392. doi:10.1242/jcs.02368
- 13) Holden HM., Ito M., Hartshorne DJ., Rayment I. (1992). X-ray structure determination of telokin, the C-terminal domain of myosin light chain kinase, at 2.8 Å resolution. *J Mol Biol*, 227(3), 841-851.
- 14) Huang, Y., & Liu, Z. (2013). Do intrinsically disordered proteins possess high specificity in protein-protein interactions? *Chemistry (Weinheim an Der Bergstrasse, Germany)*, 19(14), 4462-4467. doi:10.1002/chem.201203100; 10.1002/chem.201203100

- 15) Ikebe M., Hinkins S., Hartshorne DJ. (1983). Correlation of intrinsic fluorescence and conformation of smooth muscle myosin. *J Biol Chem*, 258(24) doi:14770-3.
- 16) Jensen, M. R., Ruigrok, R. W., & Blackledge, M. (2013). Describing intrinsically disordered proteins at atomic resolution by NMR. *Current Opinion in Structural Biology*, doi:10.1016/j.sbi.2013.02.007; 10.1016/j.sbi.2013.02.007
- 17) Jung, H. S., Billington, N., Thirumurugan, K., Salzameda, B., Cremona, C. R., Chalovich, J. M., . . . Knight, P. J. (2011). Role of the tail in the regulated state of myosin 2. *Journal of Molecular Biology*, 408(5), 863-878.
doi:10.1016/j.jmb.2011.03.019; 10.1016/j.jmb.2011.03.019
- 18) Kai F, D. R. (2013). Prostate cancer cell migration induced by myopodin isoforms is associated with formation of morphologically and biochemically distinct actin networks.. *Fasebj*, 27(12) doi:10.1096/fj.13-231571
- 19) Katayama, E., Scott-Woo, G., & Ikebe, M. (1995). Effect of caldesmon on the assembly of smooth muscle myosin. *The Journal of Biological Chemistry*, 270(8), 3919-3925.
- 20) Khaymina, S. S., Kenney, J. M., Schroeter, M. M., & Chalovich, J. M. (2007). Fesselin is a natively unfolded protein. *Journal of Proteome Research*, 6(9), 3648-3654. doi:10.1021/pr070237v
- 21) Kolakowski, J., Wrzosek, A., & Dabrowska, R. (2004). Fesselin is a target protein for calmodulin in a calcium-dependent manner. *Biochemical and Biophysical Research Communications*, 323(4), 1251-1256. doi:10.1016/j.bbrc.2004.08.224
- 22) Kosterin, S. O., Miroshnychenko, M. S., Pryluts'kyi, I., Davydovs'ka, T. L., & Tsybaliuk, O. V. (2002). Mathematical model of trans-sarcomere exchange of

calcium ions and Ca²⁺-dependent control of smooth muscle contractile activity.

[Matematychna model' transsarkolemnoho obminu ioniv kal'tsiu ta Ca²⁺-zaleznoho kontroliu skorotlivoi aktyvnosti hladen'koho m'iaza] Ukrainskii Biokhimicheskii Zhurnal, 74(2), 128-133.

23) Kudryashov DS., Vorotnikov AV., Dudnakova TV., Stepanova OV., Lukas TJ., Sellers JR., Watterson DM., Shirinsky VP. (2002). Smooth muscle myosin filament assembly under control of a kinase-related protein (KRP) and caldesmon. *J Muscle Res Cell Motil*, 23(4), 341-351.

24) Larifla, L., Deprez, I., Pham, I., Rideau, D., Louzier, V., Adam, M., . . . Teiger, E. (2012). Inhibition of vascular smooth muscle cell proliferation and migration in vitro and neointimal hyperplasia in vivo by adenoviral-mediated atrial natriuretic peptide delivery. *The Journal of Gene Medicine*, 14(7), 459-467.
doi:10.1002/jgm.2639; 10.1002/jgm.2639

25) Leinweber, B. D., Fredricksen, R. S., Hoffman, D. R., & Chalovich, J. M. (1999). Fesselin: A novel synaptopodin-like actin binding protein from muscle tissue. *Journal of Muscle Research and Cell Motility*, 20(5-6), 539-545.

26) Luther PK., Winkler H., Taylor K., Zoghbi ME., Craig R., Padrón R., Squire JM., Liu J. (2011). Direct visualization of myosin-binding protein C bridging myosin and actin filaments in intact muscle
2011 Jul 12;108(28):11423-8. doi: Proc Natl Acad Sci U S A., 108(28), 11423-11428. doi:10.1073/pnas.1103216108

- 27)Marston SB. (1989). A tight-binding interaction between smooth-muscle native thin filaments and heavy meromyosin in the presence of MgATP. *Biochem. J*, 259, 303-306.
- 28)Milton DL., Schneck AN., Ziech DA., Ba M., Facemyer KC., Halayko AJ., Baker JE., Gerthoffer WT., Cremo CR. (2011). Direct evidence for functional smooth muscle myosin II in the 10S self-inhibited monomeric conformation in airway smooth muscle cells. *Proc Natl Acad Sci U S A*, 108(4)
doi:10.1073/pnas.1011784108
- 29)Ngai, P. K., & Walsh, M. P. (1985). Properties of caldesmon isolated from chicken gizzard. *The Biochemical Journal*, 230(3), 695-707.
- 30)Onishi H., Suzuki H., Nakamura K., Takahashi K., Watanabe S. (1978). Adenosine triphosphatase activity and "thick filament" formation of chicken gizzard myosin in low salt media. *S. J. Biochem*, 83, 835-847.
- 31)Pak C., Flynn K., Bamberg J. (2008). Actin-binding proteins take the reins in growth cones. *Nature Reviews*, 9, 136-147. doi:10.1038/nrn2236
- 32)Paulin, D., Huet, A., Khanamyrian, L., & Xue, Z. (2004). Desminopathies in muscle disease. *The Journal of Pathology*, 204(4), 418-427.
doi:10.1002/path.1639
- 33)Pham, M., & Chalovich, J. M. (2006). Smooth muscle alpha-actinin binds tightly to fesselin and attenuates its activity toward actin polymerization. *Journal of Muscle Research and Cell Motility*, 27(1), 45-51. doi:10.1007/s10974-005-9053-2
- 34)Renegar, R. H., Chalovich, J. M., Leinweber, B. D., Zary, J. T., & Schroeter, M. M. (2009). Localization of the actin-binding protein fesselin in chicken smooth

muscle. *Histochemistry and Cell Biology*, 131(2), 191-196. doi:10.1007/s00418-008-0508-6; 10.1007/s00418-008-0508-6

35) Roman, H. N., Zitouni, N. B., Kachmar, L., Ijpma, G., Hilbert, . (2013).

Unphosphorylated calponin enhances the binding force of unphosphorylated myosin to actin.

Biochim. Biophys. , 4634-4641.

36) Schroeter, M., & Chalovich, J. M. (2004). Ca²⁺-calmodulin regulates fesselin-induced actin polymerization. *Biochemistry*, 43(43), 13875-13882.

doi:10.1021/bi0487490

37) Schroeter, M. M., Beall, B., Heid, H. W., & Chalovich, J. M. (2008). The actin binding protein, fesselin, is a member of the synaptopodin family. *Biochemical and Biophysical Research Communications*, 371(3), 582-586.

doi:10.1016/j.bbrc.2008.04.134; 10.1016/j.bbrc.2008.04.134

38) Schroeter, M. M., Beall, B., Heid, H. W., & Chalovich, J. M. (2008). In vitro characterization of native mammalian smooth-muscle protein synaptopodin 2.

Bioscience Reports, 28(4), 195-203. doi:10.1042/BSR20080079;

10.1042/BSR20080079

39) Schroeter, M. M., & Chalovich, J. M. (2005). Fesselin binds to actin and myosin and inhibits actin-activated ATPase activity. *Journal of Muscle Research and Cell Motility*, 26(4-5), 183-189. doi:10.1007/s10974-005-9009-6

doi:10.1007/s10974-005-9009-6

40) Shinohara, S., Kihara, T., Sakai, S., Matsusaki, M., Akashi, M., Taya, M., & Miyake, J. (2013). Fabrication of in vitro three-dimensional multilayered blood vessel model using human endothelial and smooth muscle cells and high-

- strength PEG hydrogel. *Journal of Bioscience and Bioengineering*,
doi:10.1016/j.jbiosc.2013.02.013; 10.1016/j.jbiosc.2013.02.013
- 41) Sit S., M. E. (March 1, 2011). Rho GTPases and their role in organizing the actin cytoskeleton. *Journal of Cell Science*, 124, 679-683. doi:10.1242/jcs.064964
- 42) Somlyo AP., S. A. (1981). Effects and subcellular distribution of magnesium in smooth and striated muscle. *Fed Proc*, 40(12), 2667-2671.
- 43) Song, J., & Singh, M. (2013). From hub proteins to hub modules: The relationship between essentiality and centrality in the yeast interactome at different scales of organization. *PLoS Computational Biology*, 9(2), e1002910. doi:10.1371/journal.pcbi.1002910; 10.1371/journal.pcbi.1002910
- 44) Stanek, J., Saxena, S., Geist, L., Konrat, R., & Kozminski, W. (2013). Probing local backbone geometries in intrinsically disordered proteins by cross-correlated NMR relaxation. *Angewandte Chemie (International Ed.in English)*, doi:10.1002/anie.201210005; 10.1002/anie.201210005
- 45) Stevenson R., Veltman D., Machesky L. (March 1, 2012). Actin-bundling proteins in cancer progression at a glance. *Journal of Cell Science*, 125, 1073-1079. doi:10.1242/jcs.093799
- 46) Suzuki H., Onishi H., Takahashi K., Watanabe S. (1978). Structure and function of chicken gizzard myosin. *J. Biochem. (Tokyo)*, 84, 1529-1542.
- 47) Tkatchenko A., Piétu G., Cros N., Gannoun-Zaki L., Auffray C., Léger J., Dechesne C. (2001). Identification of altered gene expression in skeletal muscles from duchenne muscular dystrophy patients.. *Neuromuscul Disord.*, 11(3), 269-277. doi:10.1016/S0960-8966(00)00198-X

- 48)Tolg, C., Ahsan, A., Dworski, S., Kirwan, T., Yu, J., Aitken, K., & Bagli, D. J. (2013). Pathologic bladder microenvironment attenuates smooth muscle differentiation of skin derived precursor cells: Implications for tissue regeneration. *PloS One*, 8(4), e59413. doi:10.1371/journal.pone.0059413; 10.1371/journal.pone.0059413
- 49)Trybus KM., Huiatt TW., Lowey S. (1982). A bent monomeric conformation of myosin from smooth muscle. *Proc Natl Acad Sci U S A*, 79(20), 6151-6155.
- 50)Trybus, K. M., & Lowey, S. (1987). Assembly of smooth muscle myosin minifilaments: Effects of phosphorylation and nucleotide binding. *The Journal of Cell Biology*, 105(6 Pt 2), 3007-3019.
- 51)Woledge, R. C., Curtin, N. A., & Rall, J. A. (2003). Molecular and cellular aspects of muscle contraction. general discussion part III. *Advances in Experimental Medicine and Biology*, 538, 671-81, 687-8.
- 52)Zhang T., Birbrair A., Wang Z., Taylor J., Messi M., Delbono O. (April 2013). Troponin T nuclear localization and its role in aging skeletal muscle. *Age*, 35(2), 353-370. doi:10.1007/s11357-011-9368-4

Appendix A: Reduction of actin-myosin dissociation by caldesmon compared to fesselin

To determine the effect of fesselin on the stability of actin-myosin Dr. Joseph Chalovich performed ATP chase experiments. 0.2 mM ATP was rapidly mixed with actin-myosin complexes in a stopped-flow spectrometer and the dissociation kinetics were followed using light scattering. Actin-myosin was rapidly mixed with ATP as seen in figure 30 (curve 1). This experiment monitored the changes in the scattered light to determine the changes in particle size.

The initial experiment with actin and myosin was repeated with the addition of 1 μM caldesmon (curve 2). The figure shows that the effect of adding the caldesmon is a decrease in the rate of light scattering change. This was interpreted as a decrease in the dissociation of the myosin from actin. Caldesmon reduced the rate of dissociation to 10% of the initial rate. The same experiment was then repeated with 1 μM fesselin added to the actin and myosin (curve 3). When this is compared with the actin-myosin alone there is on the order of a thousand-fold decrease in the rate. From this initial observation it was clear that fesselin had a much greater effect on actin and myosin interaction than caldesmon.

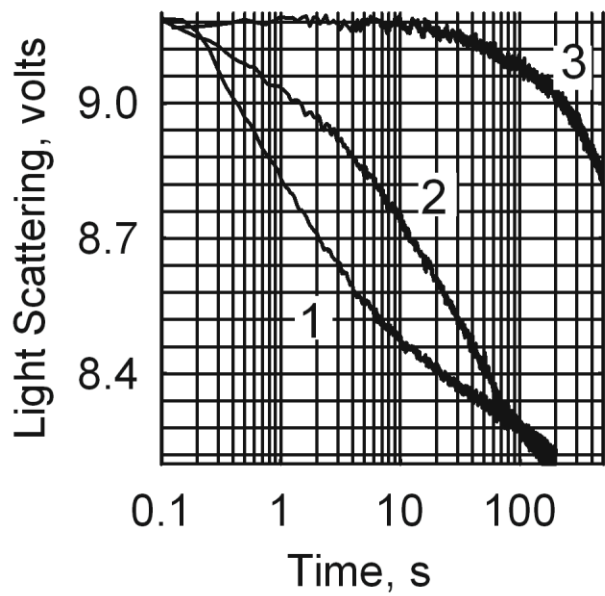


Figure 32

Fesselin slows the dissociation of actin-myosin by ATP to a greater extent than caldesmon. 1) 0.2 μM phalloidin-actin with 0.05 μM smooth myosin + 0.2 mM ATP 2) 0.2 μM phalloidin-actin with 0.05 μM smooth myosin and 0.2 μM caldesmon + 0.2 mM ATP 3) 0.2 μM phalloidin-actin with 0.05 μM smooth myosin with 0.2 μM fesselin + 0.2 mM ATP. These transients were collected on a stopped-flow measuring light scattering. Conditions: 94 mM NaCl, 10 mM MOPS pH 7.0, 2 mM MgCl_2 , 1 mM dithiothreitol, 10°C

Appendix B: Permission letter



RightsLink®

Home

Create Account

Help



ACS Publications
MOST TRUSTED. MOST CITED. MOST READ.

Title: Avian Synaptopodin 2 (Fesselin) Stabilizes Myosin Filaments and Actomyosin in the Presence of ATP
Author: Nathaniel L. Kingsbury, Randall H. Renegar, and Joseph M. Chalovich
Publication: Biochemistry
Publisher: American Chemical Society
Date: Oct 1, 2013
Copyright © 2013, American Chemical Society

User ID
<input type="text"/>
Password
<input type="text"/>
<input type="checkbox"/> Enable Auto Login
<input type="button" value="LOGIN"/>
Forgot Password/User ID?
If you're a copyright.com user, you can login to RightsLink using your copyright.com credentials. Already a RightsLink user or want to learn more?

PERMISSION/LICENSE IS GRANTED FOR YOUR ORDER AT NO CHARGE

This type of permission/license, instead of the standard Terms & Conditions, is sent to you because no fee is being charged for your order. Please note the following:

- Permission is granted for your request in both print and electronic formats, and translations.
- If figures and/or tables were requested, they may be adapted or used in part.
- Please print this page for your records and send a copy of it to your publisher/graduate school.
- Appropriate credit for the requested material should be given as follows: "Reprinted (adapted) with permission from (COMPLETE REFERENCE CITATION). Copyright (YEAR) American Chemical Society." Insert appropriate information in place of the capitalized words.
- One-time permission is granted only for the use specified in your request. No additional uses are granted (such as derivative works or other editions). For any other uses, please submit a new request.

If credit is given to another source for the material you requested, permission must be obtained from that source.

Copyright © 2014 [Copyright Clearance Center, Inc.](#) All Rights Reserved. [Privacy statement.](#)
Comments? We would like to hear from you. E-mail us at customercare@copyright.com

